UNITED NATIONS UNIVERSITY
GEOTHERMAL TRAINING PROGRAMME
Orkustofnun, Grensásvegur 9,
IS-108 Reykjavík, Iceland

Reports 2010
Number 6

ANALYSIS OF TEMPERATURE AND PRESSURE CHARACTERISTICS OF THE HVERAHLÍD GEOTHERMAL FIELD IN THE HENGILL GEOTHERMAL SYSTEM, SW-ICELAND

Misghina Afeworki Okbatsion
Ministry of Energy and Mines
Department of Mines
213 Liberty Avenue, Asmara, P.O. Box 272
ERITREA
msgn_afe@yahoo.com

ABSTRACT

The Hverahlíd geothermal field is a high-temperature field located in the southern part of the Hengill geothermal system. Interglacial lava series dominate the geological succession at Hverahlíd with subordinate sub glacial hyaloclastites. Very active northeast trending fissure swarms with northwest trending transform structures are believed to supply the main permeability for geothermal fluid flow in the area. Analysis of temperature and pressure profiles from four boreholes reveals the presence of three major feed zones at 800, 1000-1200 and 1800-2000 m depths. The reservoir at Hverahlíd geothermal field is characterised by formation temperatures of more than 300°C and pressures well over 85 bars at the best feed zones. The main up-flow zone is located in the middle of the area with a northwest directed lateral flow. A homogenous reservoir model with constant pressure boundaries fits best in simulating the injection well tests of three boreholes in Hverahlíd. The reservoir is characterised by high transmissivity and storativity values; injectivity index values comparable to the average values in the Hellisheidi area were obtained.

1. INTRODUCTION

This paper is written in partial fulfilment of the requirements of the six months geothermal training programme in UNU/GTP-2010. The report discusses the main findings and outcomes of temperature and pressure data analysis of the geothermal system at Hverahlíd, Hengill area, SW-Iceland.

Iceland is an island located in the northern part of the Atlantic Ocean. The country is situated in the middle of the Atlantic Ocean and resides on top of the northern Mid-Atlantic Ridge. The Mid-Atlantic Ridge is a divergent plate boundary and marks the locus of points along which the North American plate and the Eurasian plate are drifting away from each other in the northern part of the Atlantic Ocean. These plates are diverging at a relative motion of 2 cm/year (Björnsson, 2004). Iceland is formed as a result of extensive volcanism along this ridge and offers the only sub-aerial exposure of the ridge. Enhanced magmatic and tectonic activity in the Icelandic crust combined with rich groundwater resources from glaciers and hydrologic circulations present a unique combination of criteria for the remarkable abundance of geothermal resources in the country.

Geologically Iceland can be divided into three zones based on the age of the basaltic rocks (Iceland on the web, 2010). Tertiary flood basalts make up most of the northwest and east quadrant of the island. Quaternary flood basalts and hyaloclastites are exposed in the central and southwest parts of the island. These Quaternary rocks are cut by distinct volcanic zones; areas of active rifting that contain most of the active volcanoes. Fissure swarms make up most of the volcanic zone. These volcanic zones comprise about one-third of the area of Iceland and it is mainly in these zones that most of the high-temperature geothermal systems reside. Three main active volcanic zones (Figure 1) have been recognized in Iceland: the south-western, eastern and northern volcanic zones (Níelsson and Franzson, 2010). The Hengill geothermal or volcanic system comprises the Hengill central volcano and several geothermal fields like the Hellisheidi and Nesjavellir fields from where currently a total of 330MWe is being produced (Árnason et al., 2010). This enormous geothermal system is part of the south-western volcanic zone. The main focus of this project, the Hverahlíd geothermal field, forms the southern part of the Hengill geothermal system. The intention in this paper is to present a characterisation of the geothermal reservoir in Hverahlíd based on analysis of temperature and pressure profiles measured in four boreholes (HE-21, HE-36, HE-53 and HE-54) and analysis of several injection well tests conducted in three of these boreholes (HE-36, HE-53 and HE-54).

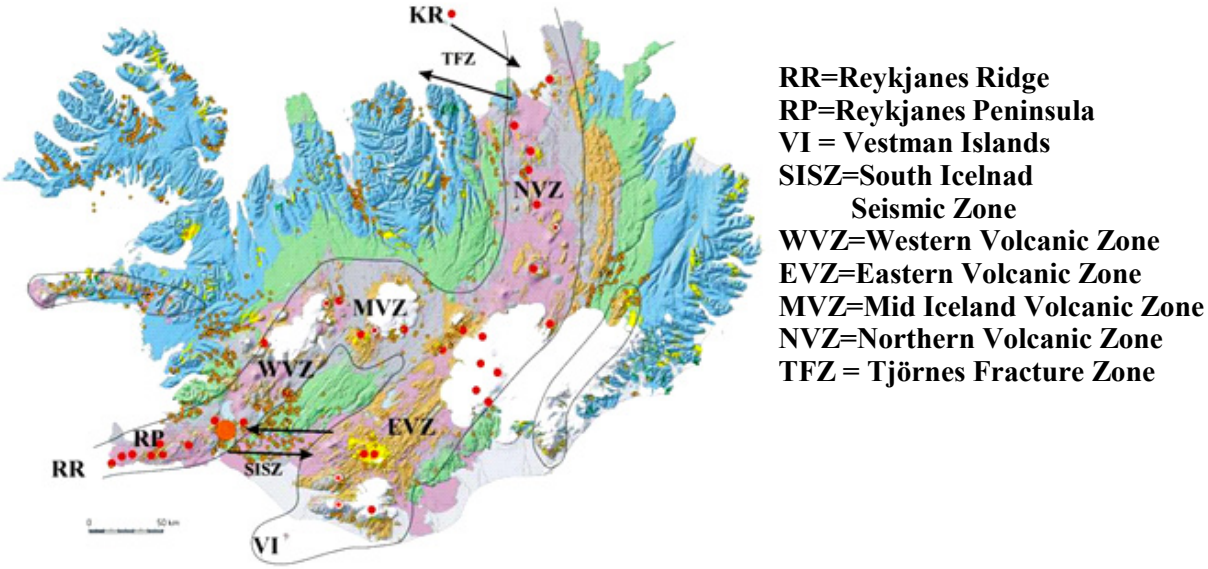

FIGURE 1: A simplified tectonic map of Iceland; orange circle shows location of the Hengill geothermal system, red/dark dots indicate high-temperature areas and white areas are glaciers (modified from Hardarson et al., 2010)

1.1 Organization of the report

In this paper a step by step insight is given into the different aspects of the Hverahlíd geothermal field. In Section 2 the focus is on describing the geology of Hverahlíd geothermal field, in association with a brief description of the geology of the Hengill geothermal system to provide a broader perspective of the geology in the area. Furthermore, some geophysical studies conducted in the area are introduced. These are intended to provide an insight into the preliminary geological model of the geothermal system.

In Section 3, the geothermal reservoir is analysed by means of different temperature and pressure measurements and profiles. An interpretation of the temperature and pressure profiles from four boreholes shows the different feed zones present in the wells. Based on these profiles an attempt was also made to give an estimate of the formation temperature and pressures in the four boreholes. Two-dimensional cross-sections to show the distribution of temperature and pressure in the geothermal reservoir are presented. This is aimed at providing better visualization of the flow patterns, up-flow

zones and cooling zones in the geothermal reservoir. Section 4 presents a description of several parameters resulting from well test analysis. A number of injection tests were done in all of the boreholes at Hverahlíd. ISOR's WellTester software (Júlíusson et al., 2008) was used to analyse the injection tests and various pressure and reservoir models are discussed. Section 5 deals with production well testing by giving a brief discussion of the theoretical background of production well testing and a description of the characteristic well curves that were drawn by Reykjavik Energy (Sigfússon et al., 2010). Finally the report presents the conclusions drawn and a summary of the outcomes of all the data analyses done.

1.2 Location and description of the study area

The Hverahlíd high-temperature geothermal field is located in the southwest part of Iceland, in the southern part of the Hengill geothermal system (Figure 2). Hverahlíd is located about 30 km east of Reykjavik, the capital. The area is characterised by gently rolling grassy or rocky plains bound by the fault scraps of the Hengill central volcano towards the west. Hengill is the highest peak in the area rising above the surrounding plains. The Hverahlíd area is easily accessible due to the fact that it is located near one of the major highways in the country that runs to the southern parts of Iceland. Two power plants are already operated in the Hengill geothermal system and a third one is planned at Hverahlíd. The Nesjavellir power plant is located north of Hengill (Figure 2) and the Hellisheidi power plant northwest of Hverahlíd. Both of these are electrical power stations and the former one is operated as a combined power plant, producing both hot water for direct use, i.e. for district heating, and electricity.

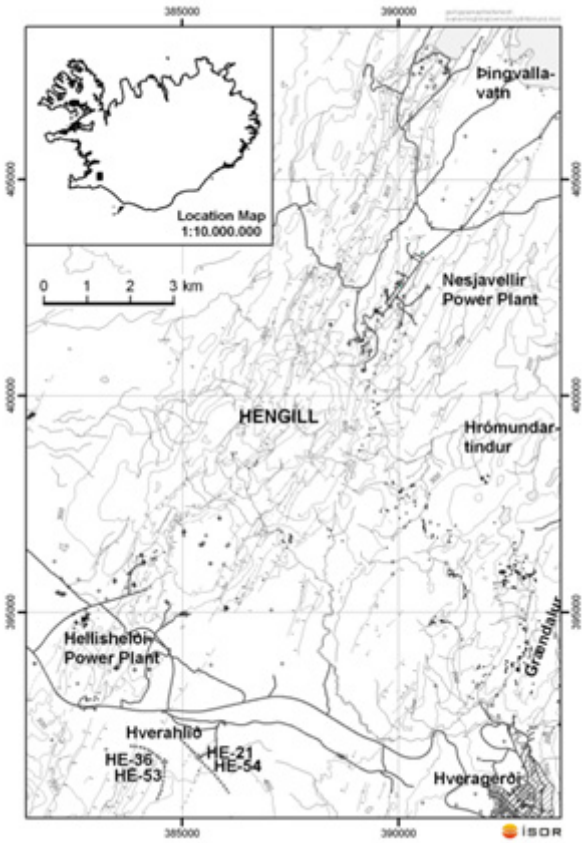

FIGURE 2: Location map of Hverahlíd geothermal field and the Hengill geothermal system

2. BACKGROUND

This chapter focuses on describing the geology of the Hverahlíd geothermal area, in association with a brief description of the geology of the Hengill geothermal system. A brief review of surface geophysical studies conducted in the area is included as well to provide a broader perspective of the geology in the area.

2.1 Geology of Hverahlíd and the Hengill area

Níelsson and Franzson (2010) describe the Hengill area as being situated at a triple junction where two active rift zones (the Reykjanes Peninsula volcanic zone and the western volcanic zone) meet a seismically active transform zone (the South Iceland seismic zone). Figure 1 shows the different volcanic zones of Iceland with respect to the Hengill geothermal system. The dominant rock formations in the Hengill area are subglacial hyaloclastites (tuffs, breccias and pillow lavas). Lava successions from interglacial periods flow to the lowlands and are therefore less common in the area (Helgadóttir et al., 2010; Níelsson and Franzson, 2010). The Hengill system is dominated by NE-SW

striking major fractures and faults. In some places, however, the fractures are intersected by easterly striking features that possibly affect the permeability of the Hellisheidi field (Hardarson et al., 2010). Volcanic fissures of 9, 5 and 2 thousand years seem to play an important role as major outflow zones in the field (Saemundsson, 1995; Björnsson, 2004; Franzson et al., 2005; and Franzson et al., 2010). The geothermal activity at the Hengill central volcano and its fissure swarms is explained by one or more up-flow zones underneath the Hengill volcano. The up-flow is caused by buoyancy as hot intrusions in the roots of the volcano heat up groundwater. This, on the other hand, also creates a pressure-low deep under the volcano so fluids from the outer boundaries of the system recharge the up-flow (Franzson et al., 2010). These fissures have been one of the two main drilling targets in the Hellisheidi field. Large NE-SW fault structures at the western boundary of the Hengill graben, with more than 250 m total throw, have also been targeted. In addition they have also been used as targets for the reinjection wells of the area (Franzson et al., 2010, Hardarson et al., 2010).

The lithology in the Hverahlíd high-temperature field is mainly composed of two rock types: hyaloclastites and lava series. The lava series are the dominant formations and were formed during interglacial periods (Helgadóttir et al., 2010; Níelsson and Franzson, 2010). This makes Hverahlíd somewhat different to the rest of the Hengill system and Níelsson and Franzson (2010) suggest that the Hverahlíd field was outside the main volcanism of the central volcano during the glacial periods. There are two types of intrusive rocks in the Hverahlíd high-temperature system (Níelsson and Franzson, 2010): dominant fine-grained basalt intrusions and minor andesitic to rhyolitic intrusions. The fine-grained nature of the intrusions indicates that they are dykes and/or sills. The intrusions are infrequent down to about 800 m b.s.l. but become more numerous at deeper levels. Below 1600 m b.s.l. the intrusive rocks become a more dominant part of the lithological succession. A geological map cropped out from the geological map of Hengill and a modified cross-section are presented in Figure 3.

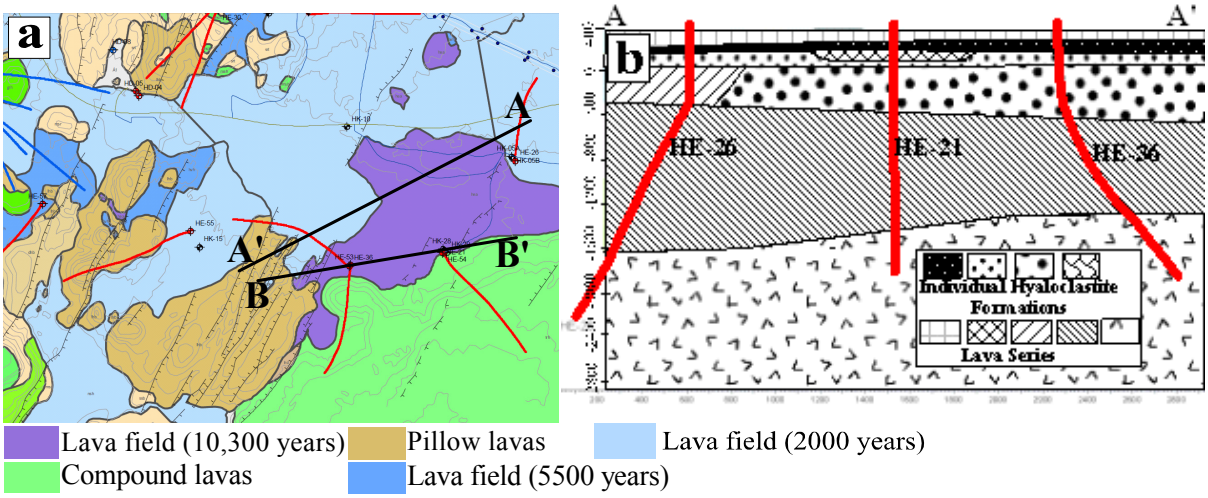

FIGURE 3: a) Geological map of the Hverahlíd geothermal field (modified from Saemundsson, 1995); b) Cross-section along line A-A' showing the geological succession at Hverahlíd (modified from Níelsson and Franzson, 2010)

2.2 Surface geophysical studies in Hverahlíd and Hengill

The surface geophysical studies for the Hverahlíd area were done in conjunction with the Hengill geothermal system. The information regarding geophysical studies presented here is from the TEM and MT resistivity surveys done by Árnason et al. (2010). Figure 4a shows the resistivity structure of Hengill geothermal system at 850 m b.s.l. A joint inversion of TEM and MT data from 148 sounding sites in the Hengill area reveals a resistivity structure consisting of a shallow low-resistivity layer in the uppermost 2 km, underlain by high resistivity. At greater depth, a second low-resistivity layer is observed in most of the area, again underlain by higher resistivity. The depth to this second low-

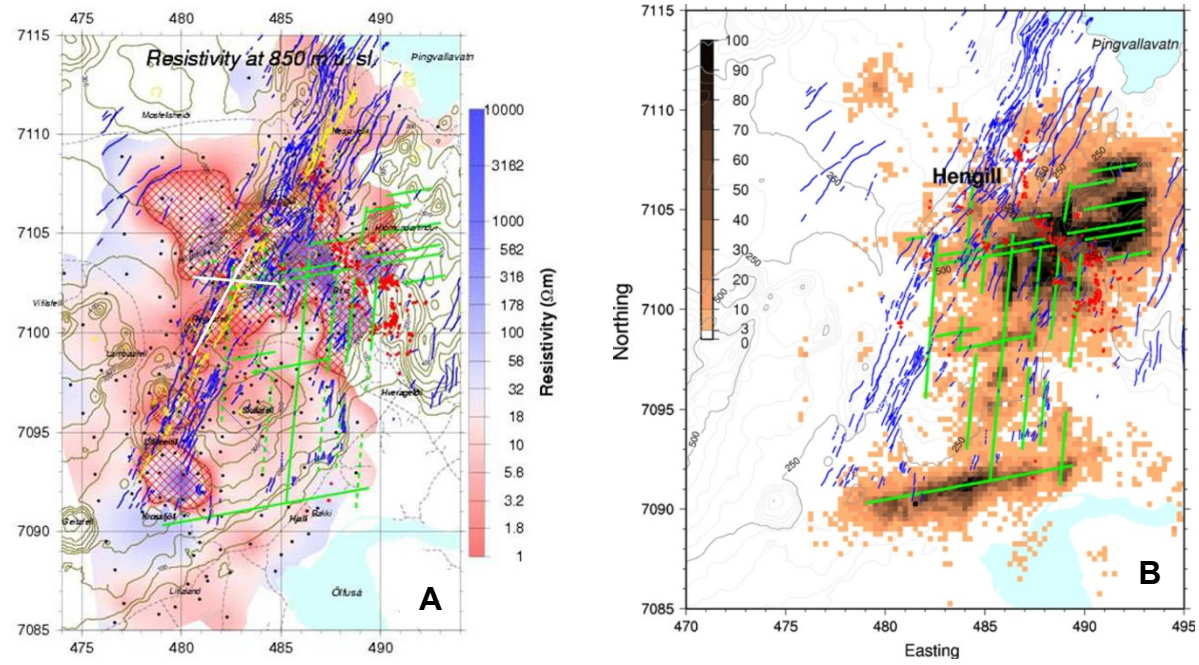

FIGURE 4: a) Resistivity at 850 m below sea level according to recent TEM surveys. High resistivity below low resistivity (< 10 Ωm) is shown as crossed lines, geothermal manifestations as red/black dots, fissures and faults as blue or brown/grey wavy lines (modified from Hardarson et al., 2010) b) Density of seismic epicentres from 1991 to 2001 and inferred transform tectonic lineaments – green/grey straight lines (modified from Árnason et al., 2010)

resistivity layer varies over the Hengill area. It is seen at the shallowest depth (about 3 km) under and around Mount Hengill. The nature of the upper low-resistivity layer is known by comparing results from MT and TEM soundings and borehole data; it reflects conductive hydrothermal alteration minerals formed at temperatures between 100 and 240°C. The nature of the deep conductive layer is not as clear, but its high conductivity could be due to magmatic brines trapped in ductile intrusive rocks. A NW–SE oriented low-resistivity anomaly through Mount Hengill and southeast of it is also seen. This anomaly is about 3.5 km wide and extends from about 3–9 km depth. Farther to the southwest, another NW–SE oriented zone of low resistivity is observed at somewhat greater depth. The low-resistivity anomalies at depth correlate with relatively positive residual Bouguer gravity, implying higher density. The NW–SE oriented, low-resistivity anomaly at 3–9 km under and to the southeast of Mount Hengill is found where intense seismic activity associated with transform tectonics occurs (Figure 4b). Since no attenuation of S-waves is observed under the Hengill area, the deep conductors are believed to reflect hot, solidified intrusions that are heat sources for the geothermal system above.

3. ANALYSIS OF TEMPERATURE AND PRESSURE PROFILES IN HVERAHLÍD

3.1 Description of the boreholes drilled in Hverahlíd

This section presents an analysis of temperature and pressure profiles that were measured in four boreholes (HE-21, HE-36, HE-53, and HE-54) in the Hverahlíd geothermal field. The locations and orientations of these 4 boreholes are shown in Figure 5 and information about the dimensions of these four boreholes is presented in Table 1 (depth values are measured borehole depths). All the information presented here was obtained from the individual drilling and well completion reports of the boreholes (Mortensen et al., 2006; Níelsson and Haraldsdóttir, 2008; Matthíasdóttir et al., 2010).

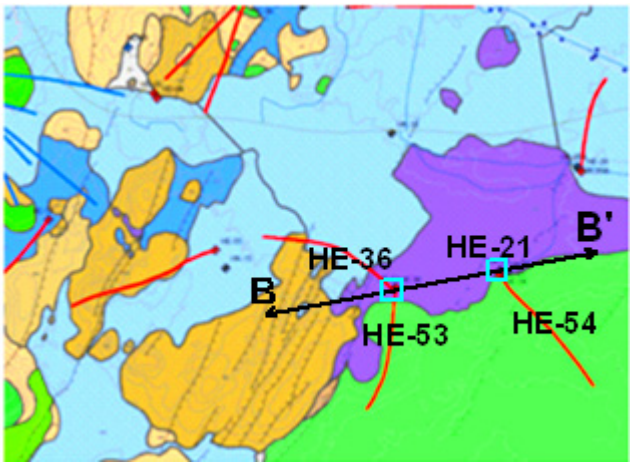

FIGURE 5: Locations and trajectories of boreholes in Hverahlíd field (background map from Saemundsson, 1995)

HE-21 was the first well drilled in the Hverahlíd area. It is vertical, drilled directly above a seismically very active fissure zone that is believed to be the feeder for the surface manifestations that are present some 200 m south of the borehole (Níelsson and Franzson, 2010). HE-54 is a directional well directed to the southeast of HE-21. HE-36 is located about 1 km west of HE-21 and is a directional well. It was targeted at exploring the presence of a geothermal reservoir associated with the active fissure swarm west of HE-21. It was directed to the northwest, so it intersects the NE-SW trending fissure swarm more or less perpendicularly. HE-53 is another directional well at the same drill site as HE-36 but with a south-southwesterly direction, so it is almost parallel to the fissure swarm.

TABLE 1: Overview of parameters for the 4 boreholes in Hverahlíd; depths are measured borehole depths with respect to the drill platform

Borehole no.	Drilled depth (m)	Casing diameter		Direction (from well head)	Casing depth	Well head coordinates (X,Y,Z)
		Surface cas. & sections 1 and 2 (″)	Slotted liner in section 3 (″)			
HE-21	2050	21, 17, 12¼	8½	Vertical	903	385379, 391644, 356
HE-36	2808	21, 17, 12¼	8½	NW	1104	384583, 391528, 353
HE-53	2507	21, 17, 12¼	8½	SSW	965	384593, 391536, 353
HE-54	2436	21, 17, 12¼	8½	SE	759	385379, 391644, 356

3.2 Interpretation of temperature and pressure profiles

Numerous temperature and pressure profiles were done in all four boreholes in Hverahlíd. The measurements were done at several stages of the drilling and after drilling with or without injection. These profiles are the main bases of the analysis presented in this chapter.

The profiles are classified into two major categories, i.e. during drilling and after drilling or warm-up profiles. Both have been used to identify the main feed zones and to analyse the flow characteristics in the reservoir. However, only the warm-up profiles were used in estimation of formation temperatures and initial pressures in the Hverahlíd geothermal field.

The measured borehole depth of the directional wells was converted to true vertical depth for the analysis of formation temperatures. This was done by projecting the measured depth into a vertical plane that hypothetically passes through the well heads of each directional borehole. Figure 6 presents selected plots of all the temperature profiles for each borehole. The ground surface is taken as a common reference point for all depth measurements in each borehole. Therefore, depth measurements relative to the drilling platform were initially corrected to become depth measurements relative to the ground surface.

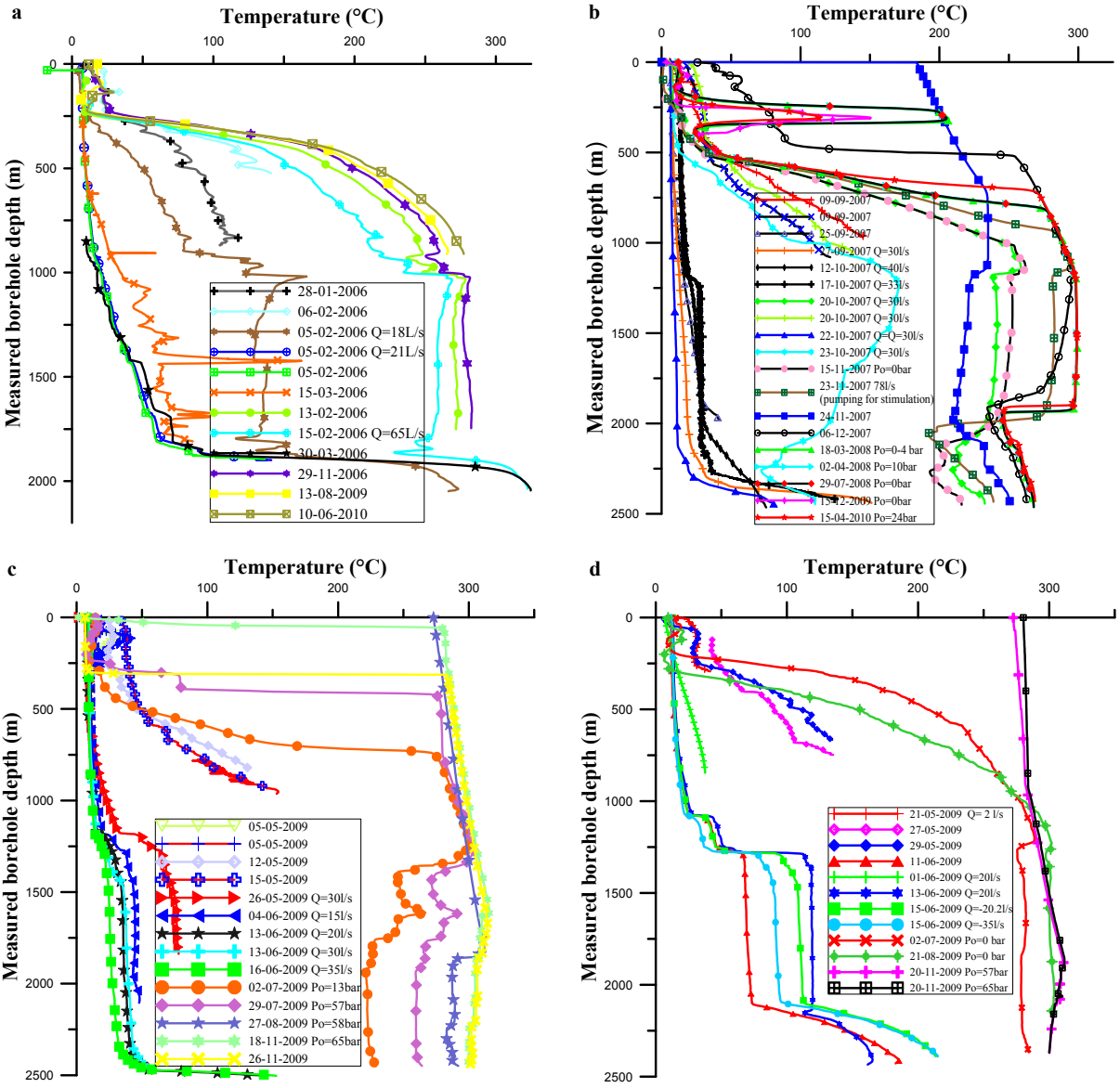

FIGURE 6: Temperature profiles of a) HE-21; b) HE-36; c) HE-53; and d) HE-54; Q = injection into the wells (L/s)

3.2.1 Borehole HE-21

More than 20 temperature profiles were measured in HE-21 (Figure 6a). The casing depth of section 2 is 903 m. Three main feed zones can be observed for this borehole at 900-1000 m depth (feed zone 1), 1400-1450 m depth (feed zone 2) and at 1850-1900 m depth (feed zone 3). The formation is apparently open below 900 m depth and enhanced cross flow between the feed zones is evident especially between feed zones 1 and 3, where the temperature profiles are straight and vertical. This cross flow of hot water seems to have a dwarfing effect on the apparently smaller feed zone 2 and other possibly minor feed zones like at 1300-1350 m and 1650-1700 m depths. This can be seen in the convective heat flow pattern in the temperature profiles taken during the warm up period.

3.2.2 Borehole HE-36

More than 35 temperature profiles were measured for HE-36 (Figure 6b) making it the most thoroughly studied and monitored borehole out of the four boreholes in this study. The production

casing depth is 1104 m (Table 1). The temperature profiles show the presence of major feed zones around 1000-1100 m (feed zone 1) and 1750-1900 m (feed zone 2) depths. Other obscured and possibly smaller feed zones are also present at 1350-1400 m and 1550 m. As in HE-21 the temperature profiles are straight and vertical between the two major feed zones, hence indicating a cross flow between them resulting in a convective heat flow profile. On the other hand, around feed zone 2, a pronounced temperature inversion is visible which could be an indication of colder water inflow into the reservoir in this zone.

An important thing to notice from the profiles is the pronounced bulging in the profiles around 200-350 m depth. This is not due to the presence of an aquifer supplying around 200°C hot fluids at such shallow depth. It is rather due to the hot fluids leaking from a ruptured casing in borehole HE-53, which is a few tens of metres away from HE-36 at this zone (Benedikt Steingrímsson, personal communication). The rupture in the casing was later repaired and consequently the following profiles do not show this bulging at the zone.

3.2.3 Borehole HE-53

About 25 temperature profiles taken at different times in the well´s history were plotted and analysed (Figure 6c). This borehole is reported to be one of the best producing wells over the entire Hellisheidi area. Some of the warm up temperature profiles clearly show why this is so. Temperatures as high as 275°C have been measured at well head, i.e. the surface, when the well head pressure was 65 bar.

The best feed zones are estimated to be at 1200-1300 m (feed zone 1), 1450-1500 m (feed zone 2), 1600-1700 m (feed zone 3) and at about 2200 m (feed zone 4). Boiling conditions or temperature values close to the boiling point curve are expected at all these feed zones. However, the warm up temperature profiles do not continue to the depth of the lowest feed zone (feed zone 4). Hence, this scenario could be debatable at this depth. Unlike boreholes HE-21 and HE-36 which took a relatively long time to heat up (one to two years after completion), this borehole appears to have attained maximum temperatures quickly (in a few months). The warm up temperature profiles appear to have stabilized. This is another indication of how quickly the reservoir has recovered from cooling. Cross flow between the feed zones is evident and there seems to be high convective heat flow at the zone where the feed zones are encountered.

After the completion of this borehole, a defective casing was discovered from the temperature profiles at 100-200 m depth. Leaking hot fluids from the ruptured casing to the surroundings heated up the formations and resulted in the anomalous temperatures measured at that zone. The casing has been repaired and the recent temperature profiles do not show these anomalous temperatures.

3.2.4 Borehole HE-54

The temperature profiles for this borehole are shown in Figure 6d. Borehole HE-54 is considered one of the best wells in the Hellisheidi - Hverahlíd area, as is HE-53. Feed zones at 700, 950, 1150-1200 and 1800-1850 m can be identified from the temperature profiles. The borehole shows an overall similarity of characteristics with HE-53, boiling at around 800 m (at 750 m for HE-53) and the feed zones seem to be at relatively similar depths. The warm up temperature profiles in this borehole also show more or less similar patterns as those from HE-53. Cross flow between the feed zones is also evident and enhanced convective heat flow is present in the zone from 950 to 1850 m in the two last measurements. In general, what has been observed for HE-53 seems also to apply for this borehole.

3.3 Estimation of formation temperature and pressure in the Hverahlíd geothermal field

Formation temperature profiles show the probable equilibrium temperatures of the rocks and the geothermal fluids in a geothermal reservoir in its initial or natural state. Circulation of drilling fluids

and the injection of cold water for cooling the well or during different injection tests (during the well completion period) significantly alter the temperature of the reservoir in the well´s vicinity. The process of estimating the equilibrium formation temperature in a well must take this into account.

After plotting the measured temperature versus the true vertical depths of the four boreholes, an idea of what the formation temperatures would look like was obtained. Here temperature profiles measured during the warm up period were used exclusively, i.e. the temperature measurements made after the final injection was finished, until the well was allowed to start blowing.

Boiling point curves were also plotted alongside the temperature profiles. The boiling point curve shows temperature and pressure values with depth assuming boiling conditions in a borehole or in a formation. The boiling point curves were calculated assuming initial water levels for each borehole at zero using the software BoilCurve (one of the programs in the ICEBOX package developed by ÍSOR, described in the ICEBOX user´s manual by Arason et al., 2004). A depth correction was then made for the calculated values with respect to the pivot point pressures and temperatures in each borehole. By doing so the actual wellhead pressures and boiling point (or saturation) temperatures were obtained.

To assist in the estimation, a Horner plot analysis of several selected depths in each well was also conducted using Berghiti, another program in the IceBox package developed by ISOR in 1993. It is a program for post-drilling thermal recovery analysis of wells, and calculates or estimates the temperatures of formations at equilibrium with boreholes (Arason et al., 2004). The formation temperature curves were then drawn by comparing and contrasting all of the aforementioned analyses. The final formation temperature and pressure plots are shown in Figures 7-10.

HE-21: The warm up temperature profiles in HE-21 show consistently increasing temperature values (Figure 7). Some of the last profiles do not reach below 900 m depth. However, the Horner plot estimates interestingly fit these profiles at the top 900 m indicating that the measured temperatures more or less reflect the formation temperatures. At lower depths, neither the temperature profiles nor the Horner plot estimates are adequate to speak confidently about the formation temperatures. However, judging from the upper 900 m, it is likely that the formation temperatures follow the same pattern, that is continuously increasing with depth but probably always below the boiling point curve. The last Horner plot point which was calculated seemed to give exaggerated temperature values. Hence, it was disregarded in the estimation as the data points used for the analysis were too few (only two). In general, the formation temperature curve shows that the temperatures in the formations are always below boiling point in this borehole, indicating liquid-dominated conditions in the reservoir.

HE-36: Adequate data is available for this borehole to make the formation temperature estimations confidently (Figure 8). The formation temperature curve shows boiling conditions in the zone at 800-1100 m depth. Pronounced temperature inversion is visible below 1700 m depth and temperatures start to rise again below 1800 m depth. Cold water inflow into the system could be the cause for this inversion. Between the boiling and the temperature inversion zones the formation temperature is straight and vertical. This indicates that convective heat flow is present in this zone due to cross flow between the feed zones found in this depth range.

HE-53 and HE-54: These wells have relatively similar formation temperature profiles. Figures 9 and 10 show the estimated formation temperature profiles and warm up profiles of HE-53 and HE-54, respectively. In both of the wells the formation temperature profiles follow the boiling point curve, especially in the zone at 750-1600 m in HE-53 and 800-1350 m in HE-54. In HE-53 the formation temperature curve shows slightly higher temperatures than the boiling point at 750-1600 m, indicating supersaturated or steam-dominated conditions in the reservoir at this level. Temperature values as high as 316°C were measured in this zone. The formation temperature profile in HE-54, on the other hand, generally conforms to the boiling point curve and slightly lower temperatures (maximum 308°C) characterise the formations in borehole HE-54.

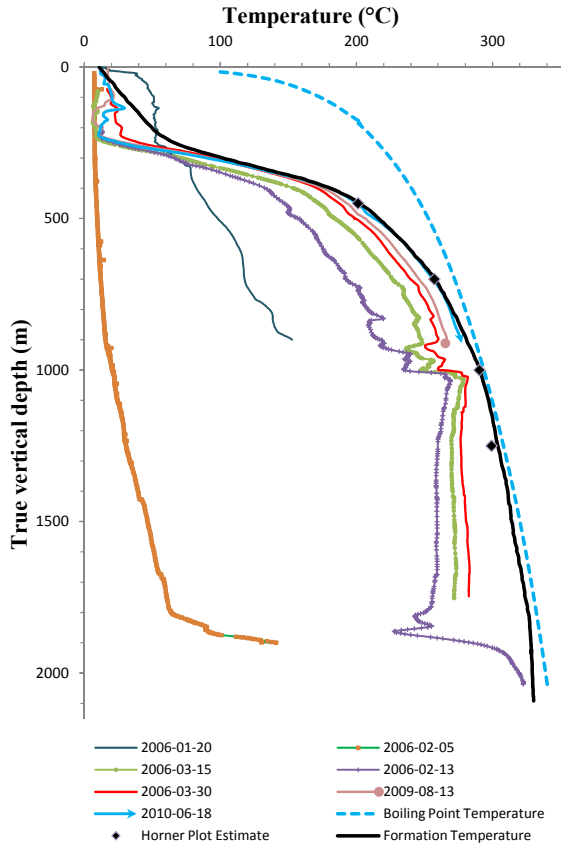

FIGURE 7: Warm up temperature profiles with the estimated formation temperature of HE-21

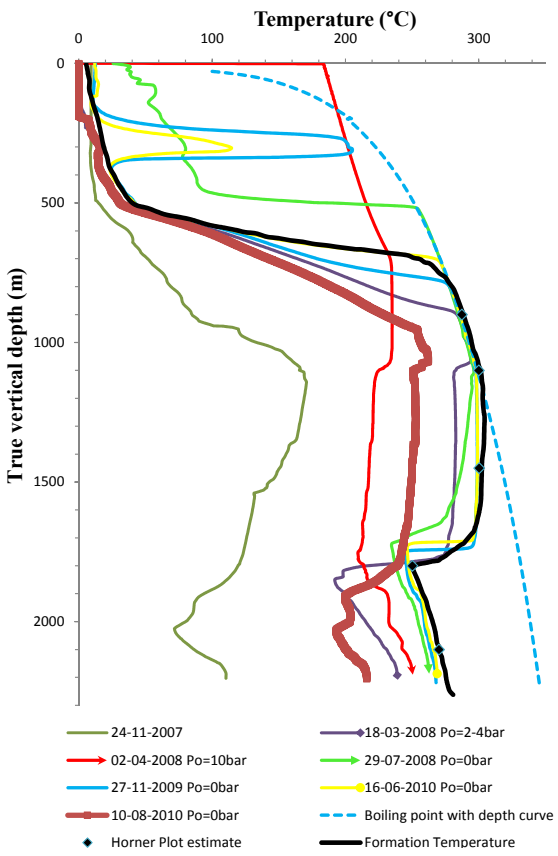

FIGURE 8: Warm up temperature profiles with the estimated formation temperature of HE-36

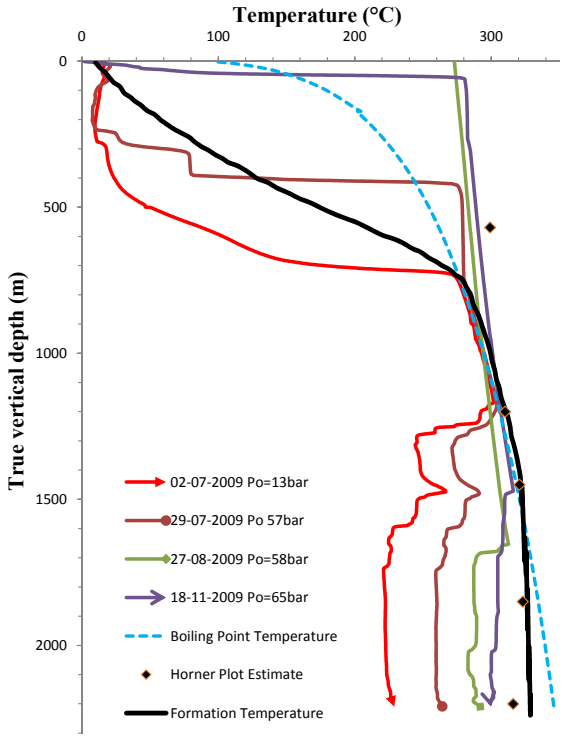

FIGURE 9: Warm up temperature profiles with the estimated formation temperature of HE-53

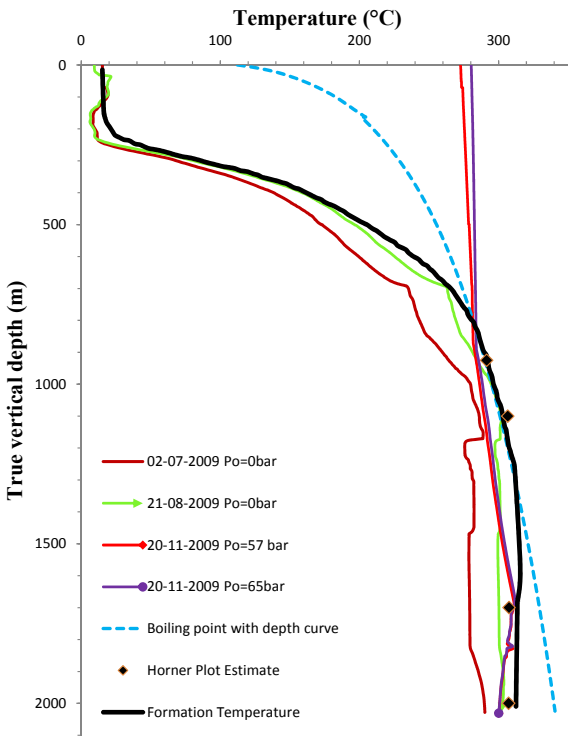

FIGURE 10: Warm up temperature profiles with the estimated formation temperature of HE-54

Figure 11 shows the plots of pressure profiles of the boreholes. They show some clear pivot points where the same pressures were measured at those same depths in many of the profiles. The boiling point with depth curves of pressure moved with respect to the depths of the pivot points. Table 2 shows a summary of the observed pivot points in each borehole.

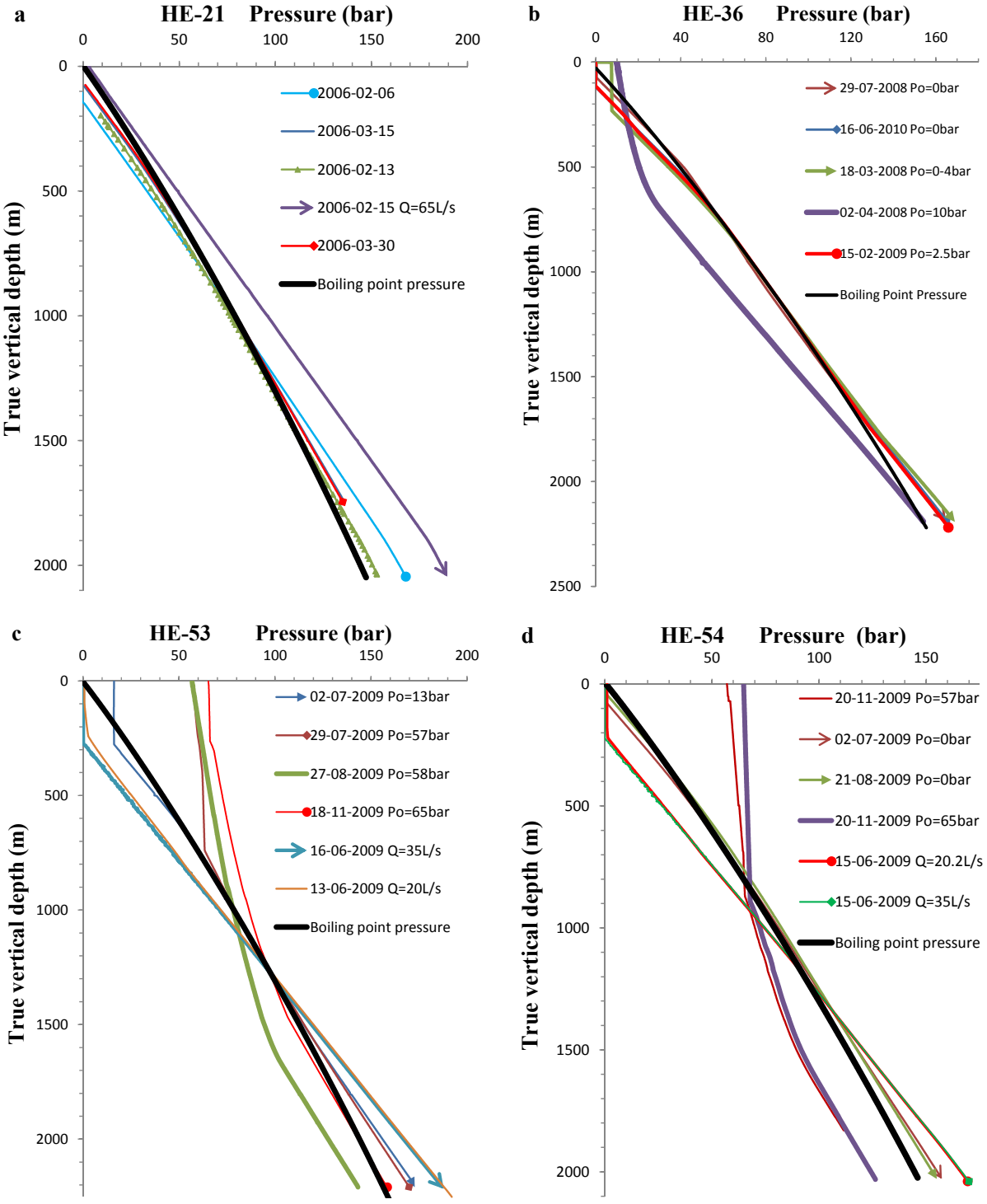

FIGURE 11: Pressure profile plots of a) HE-21; b) HE-36; c) HE-53; and d) HE-54

TABLE 2: Summary of observed pivot points

Borehole no.	No. of pivot points	Depth to pivot point (m)	Pressure at pivot point (bar)
HE-21	1	1075	85
HE-36	2	730, 1120	57, 85
HE-53	1	1264	97
HE-54	2	790, 1315	103

These pivot points show the depths and pressures at the best feed zones encountered in the respective boreholes. They can also be considered the actual pressure values from the reservoir. The main thing to notice here is the preferential occurrence of these pivot points at depth ranges 700-800 and 1000-1300 m. These two zones seem to hold the major feed zones in the Hverahlíd geothermal field as was also deduced from the temperature profiles in Section 3.2.

3.4 Two-dimensional temperature and pressure distribution in Hverahlíd geothermal field

Figure 12 shows a 2D temperature cross-section in the Hverahlíd area. It is generated from formation temperature values of the four boreholes projected to the vertical plane below the profile line B – B' in Figure 5 (Section 3.1). The profile line B – B' was chosen because it connects the wellheads of all the boreholes but mainly because it cross cuts the regional geological structures in the area more or less perpendicularly. This insures that the possible temperature variations are "seen" by the cross-section across the fault and fissure swarms present in the Hverahlíd geothermal field.

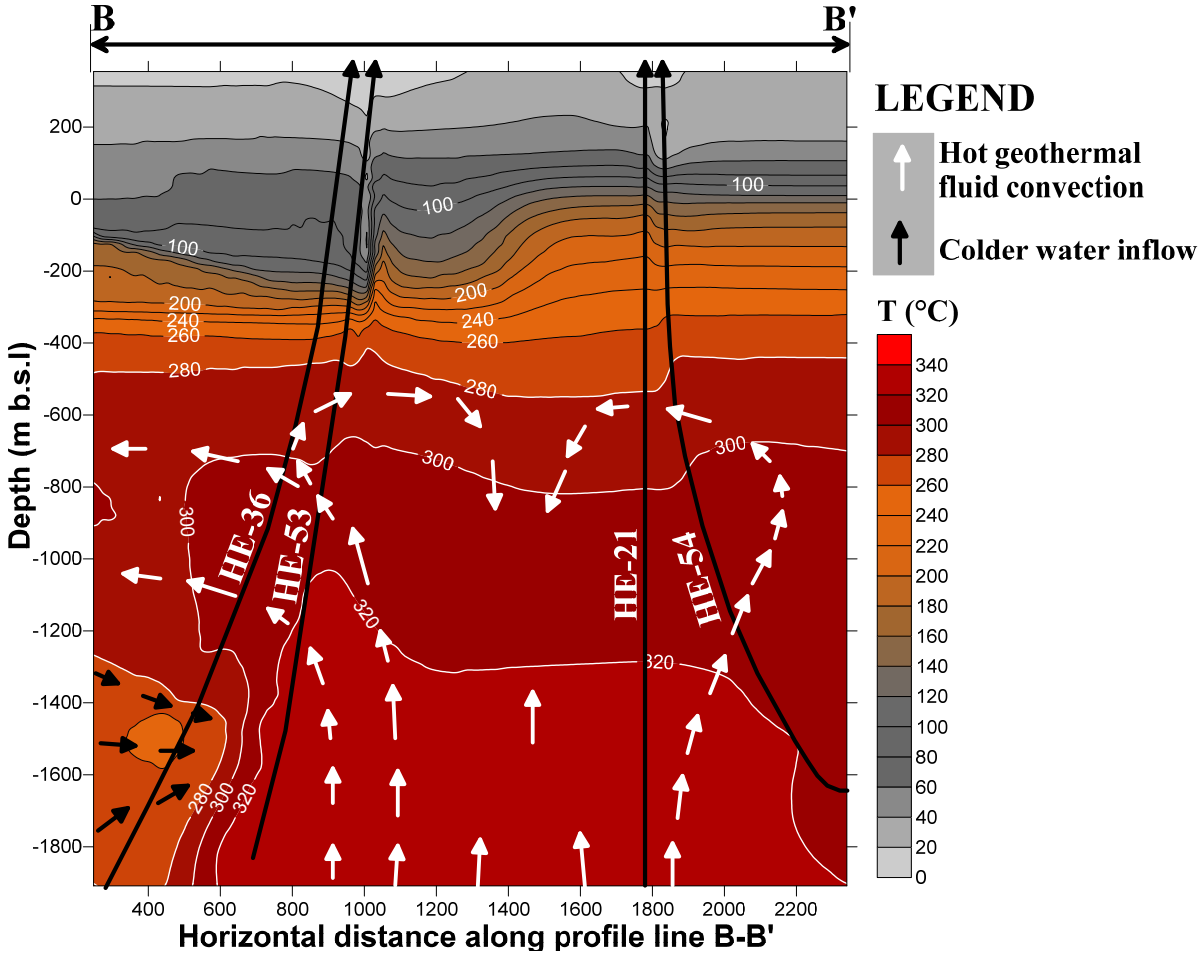

FIGURE 12: 2D temperature cross-section of Hverahlíd field

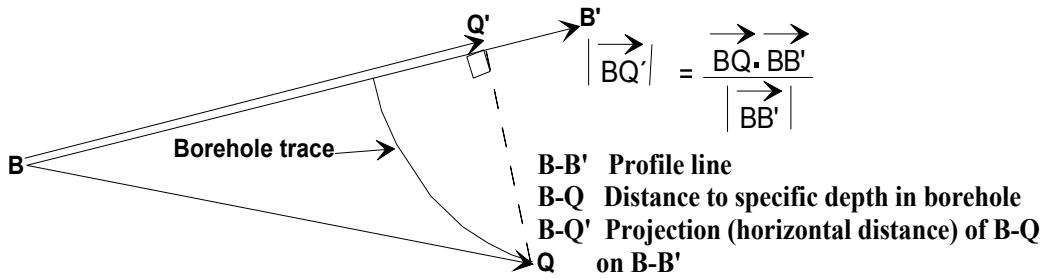

FIGURE 13: Sketch of dot product calculation of horizontal distance to profile line

Temperature values from the directional boreholes (HE-36, HE-53 and HE-54) were first projected to a hypothetical vertical plane that passes through the profile line B – B'. This can be done by means of a simple dot product of the B – B' vector and the horizontal distance of the borehole from this profile line (B – Q vector) at each depth. This can be better explained by means of the sketch in Figure 13.

After doing these calculations the outcome values were plotted in a 2D contour space (X = horizontal distance, Y = depth below sea level and Z = contour values from temperature). The programme Surfer was used and the inverse distance to power gridding method was applied for the interpolation and contouring of the 2D temperature cross-section shown in Figure 12.

The cross-section in Figure 12 shows that anomalous heat zones (>280°C) are generally found below 500 m below sea level (~700 m true vertical depth) in the Hverahlíd geothermal field. The general flow pattern is mainly upward convection in the middle of the area with pronounced northwest directed lateral flow at the depth range 750-1250 m b.s.l. (~1000-1500 m true vertical depth). This directed flow is probably controlled by the presence of NW-SE oriented transform structures in the zone (Sections 2.1 and 2.2). NW-SE oriented transform fault structures and NE-SW trending faults and fissure swarm are the main structural features believed to control the flow of geothermal fluids in Hverahlíd or even in the entire Hengill geothermal system. It is also interesting to notice that the main feed zones in the boreholes were encountered at 700-900, 1000-1300 and at 1800-2000 m (Section 3.2). Analysis of the pressure profiles (Section 3.3, Table 2) shows the presence of two pivot points at the depth range 700-1300 m, the true vertical depth. The cross-section also shows the presence of colder regions at the bottom left corner around 1400-1700 m depth range. This generally coincides with the temperature profiles of HE-36 (Figure 8) in which pronounced temperature inversion was observed at around 1700-1800 m. This can be interpreted as deep cold water inflow due to recharge from the northwest part of the area.

To generalize, a 1-1.5 km thick zone of hot water convection can be estimated from this cross-section with major feed zones around 700-900, 1000-1300 and 1800-2000 m. A reservoir thickness of 1 km can be estimated from the above analysis.

4. INJECTION WELL TESTS

4.1 Theoretical background of well test analysis

During well tests the response of a reservoir to changing production or injection is monitored. The response is governed by the characteristic properties of the reservoir such as permeability, skin effect, storage coefficient, distance to boundaries and dual porosity. Well tests are done to evaluate the properties that govern the nature of the reservoir, flow characteristics and deliverability of each well in the field. In most cases of well testing, the resulting change in pressure in the well is measured. Therefore, well test analysis is practically synonymous to pressure transient analysis (Horne, 1995)

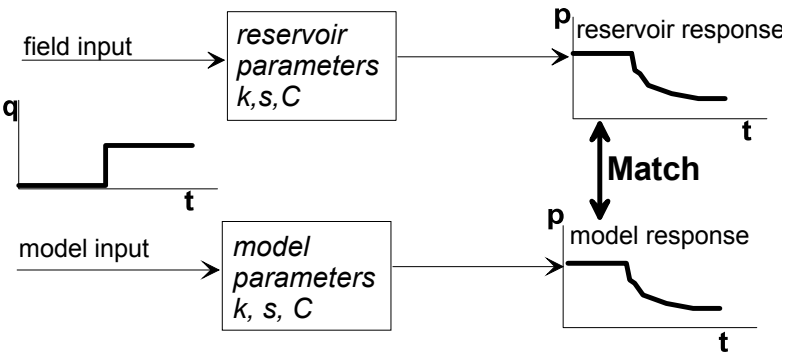

FIGURE 14: Inverse modelling applied in well test analysis (adopted from Horne, 1995)

where an input (the flow rate transient) interacts with the reservoir (the reservoir mechanism) and is detected as change in pressure - output (the pressure transient). The reservoir responses to injection or production are modelled mathematically and can be related to the actual reservoir parameters. This scenario is better illustrated by Figure 14.

The foundation for all these models is the pressure diffusion equation, which describes isothermal single-phase flow of a fluid through a porous medium (Hjartarson, 1999; Grant et al., 1982; Horne, 1995). The pressure diffusion equation, which simulates the fluid flow, may be derived by combining the conservation equations for mass and momentum with the equations of state for the fluid and the media and is expressed as Equation 1 in radial coordinates (Horne, 1995):

$$\frac{\partial^2 p}{\partial r^2} + \frac{1}{r}\frac{\partial p}{\partial r} + \frac{k_\theta}{k_r}\frac{1}{r^2}\frac{\partial^2 p}{\partial \theta^2} + \frac{k_z}{k_r}\frac{\partial^2 p}{\partial z^2} = \frac{\emptyset \mu c_t}{k_r}\frac{\partial p}{\partial t} \tag{1}$$

Several simplifying assumptions are usedwith this equation, such as:

a) Darcy's Law applies;
b) Porosity, permeabilities, viscosity and compressibility are constant;
c) Fluid compressibility is small (this equation is usually not valid for gases);
d) Pressure gradients in the reservoir are small (this may not be true in high-rate wells or for gases);
e) Flow is single phase;
f) Gravity and thermal effects are negligible.

If permeability is isotropic, and only radial and vertical flows are considered, the value of the third term on the left of Equation 1 is zero ($\frac{k_\theta}{k_r}\frac{1}{r^2}\frac{\partial^2 p}{\partial \theta^2} = 0$). In addition to this, the well testing model applied here only considers a horizontal flow, in other words pressure is only hydrostatic and varies linearly in the vertical direction, which makes the fourth term on the left of Equation 1 equal to zero ($\frac{k_z}{k_r}\frac{\partial^2 p}{\partial z^2} = 0$; i.e. the second derivative of pressure change with depth). Then Equation 1 reduces to:

$$\frac{\partial^2 p}{\partial r^2} + \frac{1}{r}\frac{\partial p}{\partial r} = \frac{\emptyset \mu c_t}{k_r}\frac{\partial p}{\partial t}, \;\; S = \phi c_t h \; and \; T = \frac{kh}{\mu} \tag{2a}$$

$$\frac{\partial^2 p}{\partial r^2} + \frac{1}{r}\frac{\partial p}{\partial r} = \frac{\mathrm{S}}{\mathrm{T}}\frac{\partial p}{\partial t}, \;\; S = \phi c_t h \; and \; T = \frac{kh}{\mu} \tag{2b}$$

Equation 2 is (according to Horne, 1995): "recognizable as the diffusion equation; solutions to this equation have been developed for wide variety of specific cases, covering many reservoir configurations". The different parameters are explained below in Equations 3 and 4.

A detailed explanation of the mathematical solutions for Equations 1 and 2 is also presented by Hjartarson (1999). It is beyond the scope of this project to describe the different models and mathematical solutions involved in determining them. It is rather practical and relevant to describe the different reservoir parameters that were analysed using the injection test data mentioned in this section.

The prime target of injection well tests is to investigate the main boundary conditions that control the response of the reservoir to pressure changes caused by the injection. The different boundary conditions and the expected responses of the reservoir can better be apprehended schematically as in Figure 15. Some important reservoir parameters that are calculated using injection well testing data are listed and described as follows:

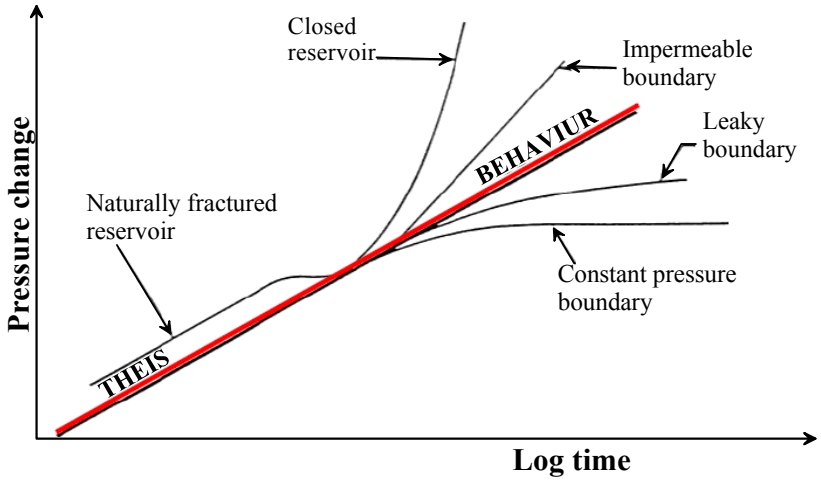

FIGURE 15: Schematic plot of logarithm of the time elapsed during injection (Log time) vs. pressure change, showing the effect of different boundary conditions and the observed responses of the reservoir. In the Theis behaviour (solution), the reservoir *behaves as if it is infinitely large,* this means boundary effects are not present. Boundary effects will, however, *eventually appear in every reservoir* (adopted from Hjartarson, 1999 and Jónsson, 2010)

Transmissivity – T (Equation 3) is an important characteristic of reservoirs and is a measure of the ability of the reservoir to transmit fluid, determining how fast the pressure changes between the well and the reservoir; SI Unit is $[\mathrm{m}^3/(\mathrm{Pa}\cdot\mathrm{s})]$:

$$T = \frac{kh}{\mu} \tag{3}$$

Storativity – S (Equation 4) is another important reservoir parameter that is defined as the volume of fluid stored in the reservoir, per unit area, per unit increase in pressure. Hence it has great impact on how fast the pressure wave can travel within the reservoir; SI unit is $[\mathrm{m}^3/(\mathrm{Pa}\cdot\mathrm{m}^2)$ or $\mathrm{m}/\mathrm{Pa}]$:

$$S = \phi c_t h \tag{4}$$

Injectivity Index – II (Equation 5) is defined as the change in the injection flow rate divided by the change in stabilized reservoir pressure. It is often used as a rough estimate of the connectivity of the well to the surrounding reservoir; SI unit is $[(\mathrm{L}/\mathrm{s})/\mathrm{bar}]$:

$$II = \left|\frac{\Delta Q}{\Delta P}\right| \tag{5}$$

Skin factor (s) is a unitless variable used to quantify the permeability of the volume immediately surrounding the well. This volume is often affected by drilling operations, being either damaged (e.g. because of drill cuttings clogging the fractures) or stimulated (e.g. due to extensive fracturing around the well). For damaged wells the skin factor is positive and for stimulated wells it is negative.

Wellbore storage (C) is a volume property (m^3) that accounts for the difference between the wellhead flow rate, and the "sand face" flow rate (i.e. the flow into or out of the actual formation).

Radius of investigation (r_e) is the approximate distance (m) at which the pressure response from the well becomes undetectable. Hence, this radius defines the area around the well being investigated. The boundary conditions seen in the data define the values of r_e, hence calculated values should be taken qualitatively. In the above equations the following definitions are valid:

μ is the dynamic viscosity of the active reservoir fluid, in Pa·s.
ϕ is the average reservoir porosity, usually expressed in percentage fractions.
c_t is the total compressibility of the rock and the reservoir fluid, in Pa^{-1}.
k is the effective permeability in m^2 but is commonly referred to using Darcy units, i.e. 1 D ≈ 10^{-12} m^2; it is a measure of the ability of the reservoir rock to transmit fluid.
h is the estimated thickness of formation that is actively exchanging fluid with the wellbore, in m.
$\Delta Q = (Q_f - Q_i)$ is the change in the injection or production rates, in L/s.
$\Delta P = (P_f - P_i)$ is the change in the observed pressure change, in Pa.

4.2 Description of ISOR's well tester programme

WellTester (WT) is a program that was written at Iceland GeoSurvey (ÍSOR) to handle data manipulation and analysis of well tests (mainly multi-step injection tests) in Icelandic geothermal fields (Júlíusson et al., 2008). The programme handles the analysis of well test data in six steps that range from setting initial conditions to modelling and finally generating a report. WellTester uses windows based graphical user interface that offers a good deal of user friendly processing of the well test data. In the first step the program allows the input of initial reservoir parameters like estimated reservoir temperature, pressure, well bore radius, porosity and automatically suggests dynamic viscosity and total compressibility. However, these two can also be input manually if their values are known from other sources. The next step is mainly about adjusting the different well testing steps and specifying the injection or production rates. Then a step for performing modification of the measured data appears. In this step different corrections and modifications can be performed on the original data, like excluding unwanted data points, adding missing data points manually, etc., so that the data is more suitable for modelling. The next step, (the modelling step) is where a model is selected and parameters can be set for modelling the observed response of the reservoir to injection or production. The flow models in WellTester are based on single-phase flow through homogeneous or dual porosity reservoirs. The reservoir fluid is assumed to be slightly (and only slightly) compressible, which further limits the applicability to single-phase liquid reservoirs and well tests where the fluid stays as single-phase liquid throughout the test. WellTester offers three types of boundary models (infinite boundary, constant pressure boundary and no flow boundary) to make the inverse calculations of different reservoir parameters (transmissivity, storativity, etc). The parameters are calculated by iterations of some initial input values in this step. Then the program transfers the process to the Model All step. This step simulates the data from all the steps based on the parameters calculated for a single step that is specified to it (usually the first step). In this step, the program tries to find the best fitting model for all the steps in one single model and comes out with an estimate of the parameters based on this best fit model. The final step is the reporting, where WT generates a report of all the inputs, processes and the calculations done in the program in a tabulated and graphical display of the values.

4.3 Results of the well test analysis: interpretation of physical reservoir parameters

Injection well test analysis was done for HE-36, HE-53 and HE-54. The injection test data was found to be inadequate for HE-21, hence, no analysis was done for this borehole. The well test models used for the injection analysis of the three boreholes are summarised in Table 3. The results of the analysis are presented below for each borehole, followed by a common overview of the results.

The injection well test analysis for the three boreholes was simulated with different boundary and reservoir models. Several iterations of the models were done for different reservoir parameters. Interestingly, however, constant pressure boundaries with homogenous reservoir models returned the best fits for all the boreholes. In a constant pressure boundary condition, pressure changes in the well stabilize and the measured pressures become constant. In other words, the time rate of change of pressure approaches zero. This phenomenon happens when the injection or production to and from a well equals recharge from the reservoir. Constant pressure boundaries are a result of the presence of

factors like injection wells and flowing fractures that cause the pressure response to reach steady state. In such cases the measured pressure in the well will be similar to the pressures at the boundary (Elíasson and Kjaran, 1983 and Jónsson, 2010). This is expected in the case of Hverahlíd geothermal field as it is characterised by presence of abundant fractures and a fissure swarm that could be connected to other reservoirs in the area.

TABLE 3: Summary of model selected for the well test analysis

Reservoir	Homogeneous
Boundary	Constant pressure
Well	Constant skin
Wellbore	Wellbore storage

WellTester requires the input of some initial parameters that will be used to calculate some deduced parameters like reservoir thickness and effective permeability. The initial parameter values need not be accurate values of the reservoir being modelled. Rough estimates are usually good enough. The initial parameter values used for this analysis are shown in Table 4 below.

TABLE 4: Summary of initial parameter values

Borehole ID	**HE-36**		**HE-53**		**HE-54**	
	Parameter	**Unit**	**Parameter**	**Unit**	**Parameter**	**Unit**
Estimated reservoir temperature (T_{est})	280	°C	280	°C	280	°C
Estimated reservoir pressure (P_{est})	154	bar	148	bar	117	bar
Wellbore radius (r_w)	0.11	m	0.11	m	0.11	m
Porosity (φ)	0.10	-	0.10	-	0.10	-
Dynamic viscosity of reservoir fluid (μ)	9.6×10^{-5}	Pa·s	9.6×10^{-5}	Pa·s	9.5×10^{-5}	Pa·s
Total compressibility (c_t)	6.4×10^{-10}	Pa^{-1}	6.4×10^{-10}	Pa^{-1}	6.5×10^{-10}	Pa^{-1}

The estimated reservoir temperature values considered in this analysis are taken from the default values given by the WellTester software. These values are derived from the overall estimated reservoir temperature in the Hellisheidi area. The same is true for the porosity, dynamic viscosity and total compressibility values.

Based on these initial parameters and the well test models summarized in Table 3, the program performed non-linear regression analysis to find the parameters that best fit the injection test data which consists of pressure versus time at a specific depth and ΔQ, i.e. the change in injection or production rate. The results of the analysis of the specified boreholes with brief discussions are presented below.

HE-36: The modelled response from the non-linear regression analysis of the observed data for "all steps" (step 1 and 2) is presented in Figure 16. Table 5 shows a summary of the injection steps in HE-36. The model fits the data quite well and can be taken as representative of reservoir response to injection. Based on this model, the different reservoir parameters that were calculated are presented in Table 6. It can be seen that the values are consistent in all the steps giving more or less accurate values of the reservoir parameters. The results of the Injectivity index calculated from the measured data are closely comparable to the injectivity index calculated from the model (Table 6).

TABLE 5: Summary of the injection steps in HE-36

Step no.	**Time (hr)**	**$\lvert Q_i - Q_{i+1} \rvert$ (L/s)**	**ΔQ (L/s)**	**ΔP (bar)**	**Injectivity index ((L/s)/bar)**
1	1.5	30 – 70	40	10	4
2	1.5	70 – 30	40	8	5

TABLE 6: Summary of results from non-linear regression parameter estimate for HE-36

Parameter name	Modelling all steps	Step 1	Step 2
Transmissivity (T) – $m^3/(Pa{\cdot}s)$	4×10^{-8}	4×10^{-8}	3.8×10^{-8}
Storativity (S) – $m^3/(Pa{\cdot}m^2)$	2×10^{-8}	2×10^{-8}	4.3×10^{-8}
Radius of investigation (r_e) – m	120	100	98
Skin factor (s)	-1.9	-1.6	-2
Wellbore storage (C) – m^3/Pa	7×10^{-6}	9×10^{-6}	5.7×10^{-6}
Injectivity index (II) – (L/s)/bar	5	5	5
Coefficient of determination %	100	99	99
Deduced reservoir thickness – m	350	670	325
Deduced effective permeability – m^2	1×10^{-14} (≈11 mD)	1×10^{-14} (≈12 mD)	5×10^{-15} (≈5 mD)

The fit between the model and collected data for all steps of HE-36 (Figure 16) shows how well the model simulates the observed pressure responses. The consistency of the calculated reservoir parameters in each step is mainly due to this good fit. Figure 17 shows the fit between model and selected data on a log-linear scale (A) and a log-log scale (B). The derivative shown on the right plot is commonly used to determine the most appropriate type of model. The derivative plot in Figure 17b is basically a time derivative of the change in pressure multiplied by time. The fact that it tends to drop to zero is typical of constant pressure boundary models. In such models (when the boundary conditions are attained in the test), pressure approaches steady state and the changes in the pressure in the well approach zero, hence the derivative plot tends to zero.

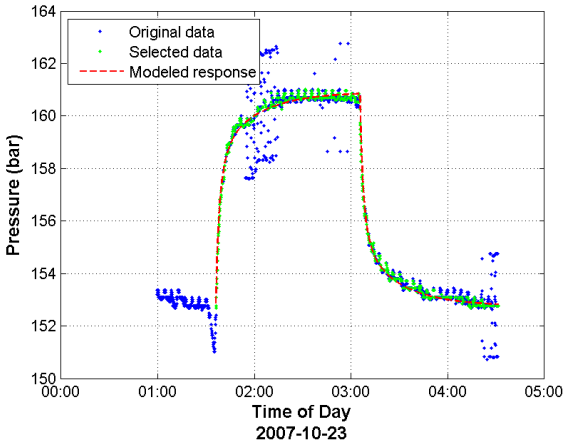

FIGURE 16: Fit between model and collected data for all steps of HE-36

From the results of the analysis, it can be observed that HE-36 is characterised by good values of transmissivity and storativity with generally average values of injectivity index (average values of II in Hellisheidi area range from 5 to 7 (L/s)/bar; Júlíusson et al., 2008). In addition, all the well test parameters shown in Table 6 are comparable to the average values of geothermal wells as a whole.

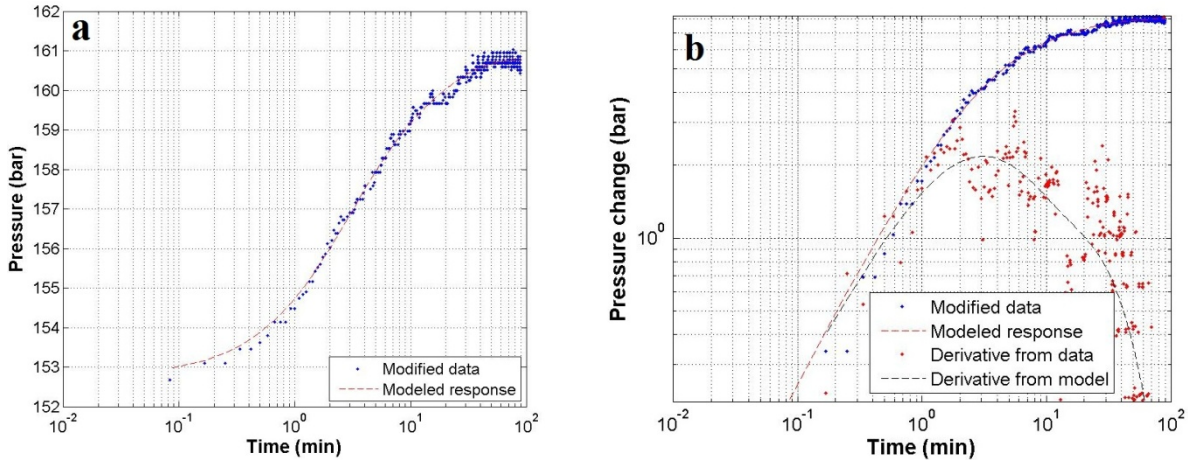

FIGURE 17: Fit between model and selected data of step 1 in HE-36 on a) log-linear scale; and b) log-log scale

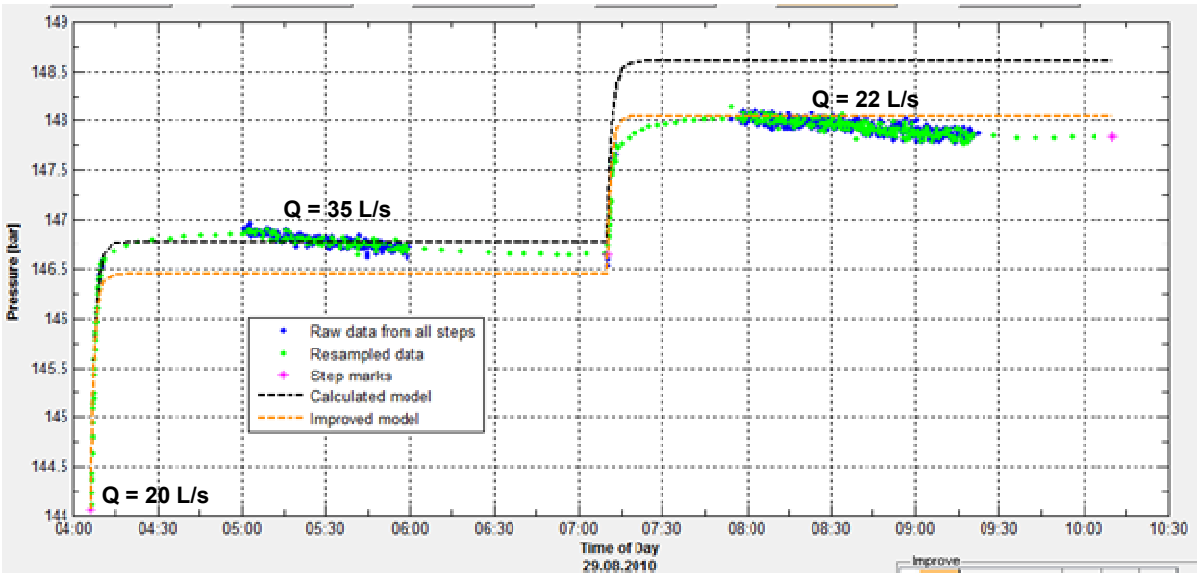

FIGURE 18: Fit between model and collected data for all steps of HE-53

HE-53: The two-step injection test in HE-53 (Figure 18) was performed after fixing the already mentioned rupture in the casing; a new casing was installed into the upper part of the well. Table 7 presents a summary of the steps of the injection test in HE-53. The best fit plots for all the steps of the test and the relevant parameters that were calculated for HE-53 are presented in Figure 18 and Table 8, respectively, while the model fits of step 1 are given in Figure 19. As can be seen from Table 7, the change in pressure due to injection in this borehole is relatively small.

TABLE 7: Summary of the injection steps in HE-53

Step no.	Time (hr)	$\|Q_i - Q_{i+1}\|$ (L/s)	ΔQ (L/s)	ΔP (bar)	Injectivity index ((L/s)/bar)
1	3	20 – 35	15	2.55	6
2	3	35 - 45	10	1.15	6.5

The measured pressure response in HE-53 showed a declining trend (Figure 18) while water was being injected into the well. This is usually not expected to happen. In injection tests, pressure responses commonly either keep on increasing or stabilize and attain steady state. The reason is probably due to the opening up of some fractures during the injection test or possibly due to interference from a nearby pressure boundary. This complicated the modelling of the pressure response, resulting in a relatively low fit between the model and the measured pressure response. The effect of minor and local fluctuations in the measured response in cases like this (small overall pressure changes) is magnified which otherwise would have been smoothed out if the overall change in pressure was larger. Taking longer steps in the test or increasing the injection rates to create larger pressure changes so that more regional boundary effects could be observed would be recommended in this kind of scenario.

The fit between the modelled injection response and the measured data of HE-53 (Figure 18) is not as good as that for HE-36. This can also be observed in the calculated parameters for this borehole presented in Table 8. All the parameters calculated for step 2 are slightly higher than those of the Model All values and those of step 1. Nevertheless, the results are comparable to the average reservoir parameters observed in Hellisheidi area.

TABLE 8: Summary of results from non-linear regression parameter estimates for HE-53

Parameter Name	Modelling all steps	Step 1	Step 2
Transmissivity (T) - $m^3/(Pa{\cdot}s)$	3×10^{-8}	2×10^{-8}	5×10^{-8}
Storativity (S) - $m^3/(Pa{\cdot}m^2)$	1×10^{-8}	2×10^{-8}	6×10^{-11}
Radius of investigation (r_e) - m	10	10	65
Skin factor (s)	-1.3	-1.4	-1.7
Wellbore storage (C) - m^3/Pa	5×10^{-6}	5×10^{-6}	8×10^{-6}
Injectivity index (II) - (L/s)/bar	6	5.5	7
Coefficient of determination %	92	97	91
Deduced reservoir thickness – m	300	375	--
Deduced effective permeability - m^2	1×10^{-14} (≈ 10 mD)	7×10^{-15} (≈ 7 mD)	5×10^{-12} (≈ 5×10^3 mD)

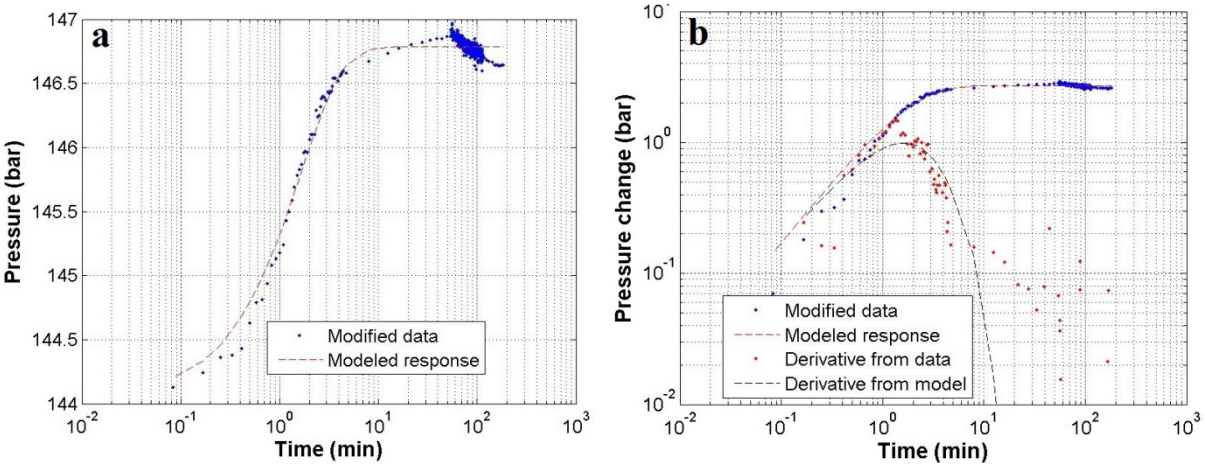

FIGURE 19: Fit between model and selected data of step 1 in HE-53 on a) log-linear scale; and b) log-log scale

HE-54: A three-step injection test was carried out and analysed for HE-54. Table 9 presents a summary of the steps of the injection test in HE-54. The best fit results for "modelling all steps" of the test and the relevant parameters that are calculated for HE-54 are presented in Figure 20 and Table 10, respectively, and the results of step 1 are shown in Figure 21.

TABLE 9: Summary of the injection steps in HE-54

Step no.	Time (hr)	$\lvert Q_i - Q_{i+1} \rvert$ (L/s)	ΔQ (L/s)	ΔP (bar)	Injectivity index ((L/s)/bar)
1	3	22-35	13	0.21	62
2	3	35-45	10	0.31	32
3	4	45-20	25	0.56	45

As was observed in HE-53, the overall changes in the pressure response were very small in all of the three steps of the injection test for HE-54, only on the order of fractions of a bar (Table 9). The injectivity index values of this well are therefore high. Considering the fact that HE-54 is one of the best producing wells in Hellisheidi area, these values are generally acceptable.

Although the fit between model and the measured data for this borehole does not seem to be good in Step 3, the model fits relatively well for the other steps. The calculated parameters also are reasonable from a practical point of view. The injectivity index values are very high compared to those from the

other boreholes. However, they are also in agreement with the values calculated from the measured pressure response (Table 9). The transmissivity in this borehole is also high indicating how effectively the reservoir can transmit water. The effective permeability as a consequence of this is also very high. This high transmissivity and effective permeability values are the main reason for the small pressure gradients measured in this borehole. This means pressure gradients in the well (during the test) were transmitted to the reservoir and the reservoir responded effectively to those changes and stabilized quickly. In such cases, pressure changes are usually small. The high injectivity index values are also a consequence of this high transmissivity. However, the overall calculated parameters are generally comparable to those commonly observed in Icelandic geothermal systems (Júlíusson et al., 2008).

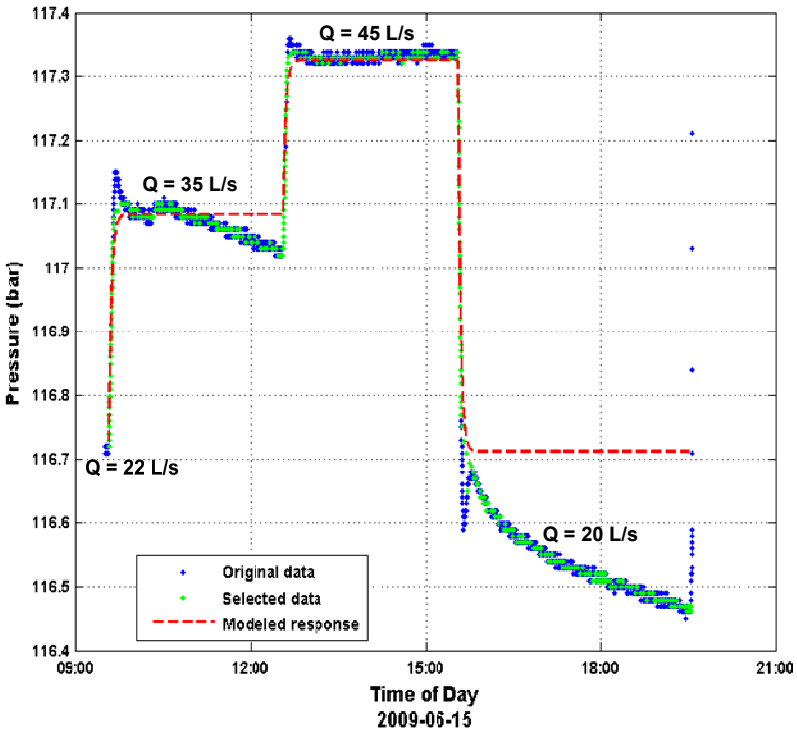

FIGURE 20: Fit between model and collected data for all steps of HE-54

TABLE 10: Summary of results from nonlinear regression parameter estimate for HE-54

Parameter name	Modelling all steps	Step 1	Step 2	Step 3
Transmissivity (T) - $m^3/(Pa{\cdot}s)$	2×10^{-7}	2×10^{-7}	4×10^{-7}	3×10^{-7}
Storativity (S) - $m^3/(Pa{\cdot}m^2)$	1×10^{-8}	3×10^{-8}	2×10^{-8}	5×10^{-8}
Radius of investigation (r_e) - m	30	20	30	750
Skin factor (s)	-2.6	-2.3	2.2	-1.5
Wellbore storage (C) - m^3/Pa	6×10^{-5}	6×10^{-5}	5×10^{-5}	5×10^{-5}
Injectivity index (II) - (L/s)/bar	35	42	34	29
Coefficient of determination %	89	89	97	97
Deduced reservoir thickness - m	215	497	762	298
Deduced effective permeability - m^2	9×10^{-14} m^2 (≈90 mD)	4×10^{-14} (≈39 mD)	1×10^{-13} m^2 (≈135 mD)	4×10^{-14} (≈39 mD)

4.4 Summary and discussion

Table 11 summarises the calculated well test parameters of the three boreholes. Values shown are those calculated in the all steps model. Also included is a foot remark of the commonly observed values in either Icelandic geothermal reservoirs or values that are generally observed in geothermal systems for the sake of comparison.

HE-54 is characterised by relatively higher values of transmissivity, storativity and injectivity indices than the other wells. From the overall geological and temperature profile observations made and discussed in Sections 2 and 3, the values of these parameters in HE-53 would be expected to be similar

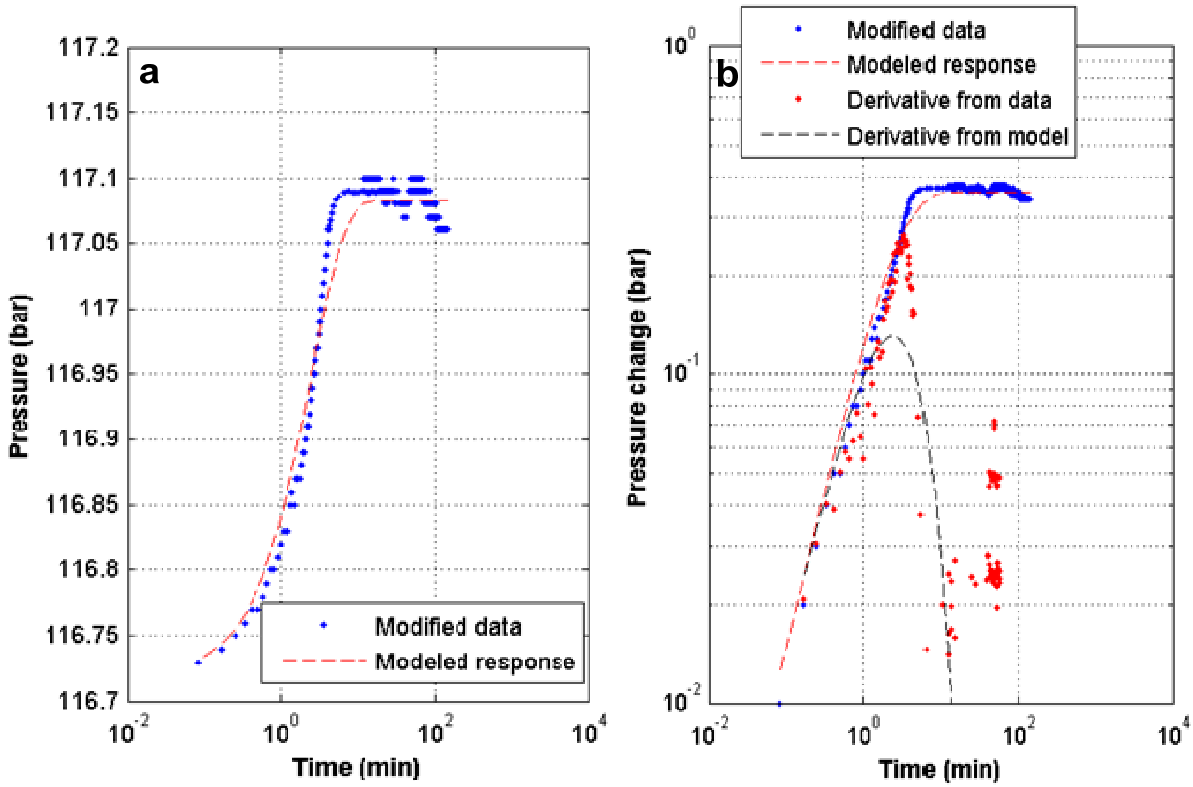

FIGURE 21: Fit between model and selected data of Step 1 in HE-54 on a) log-linear scale; and b) log-log scale

to HE-54. However the well test analysis of HE-53 showed complications due to local boundary effects, hence the parameters might not be the most accurate. On the other hand, the parameters calculated for HE-36 are based on more than 97% fit accuracy (coefficient of determination) and can be taken as representative reservoir parameters for the well.

TABLE 11: Summary of calculated parameters of all steps for the three boreholes

Parameter name	HE-36	HE-53	HE-54
Transmissivity (T) - $m^3/(Pa{\cdot}s)$	4×10^{-8}	3×10^{-8}	2×10^{-7}
Storativity (S) - $m^3/(Pa{\cdot}m^2)$	2×10^{-8}	2×10^{-8}	1×10^{-8}
Radius of investigation (r_e) - m	120	10	30
Skin factor (s)	-1.9	-1.3	-2.6
Wellbore storage (C) - m^3/Pa	7×10^{-6}	4×10^{-6}	6×10^{-5}
Injectivity index (II) - (L/s)/bar	5	6	35
Coefficient of determination %	100	92	89
Deduced reservoir thickness - m	350	300	200
Deduced effective permeability - m^2	1×10^{-14} (≈11 mD)	1×10^{-14} (≈10 mD)	9×10^{-14} (≈90 mD)

Júlíusson et al. (2008), states that for Icelandic geothermal reservoirs transmissivity T is on the order of 10^{-8} [$m^3/(Pa{\cdot}s)$]; that common values of storativity S for liquid-dominated geothermal reservoirs are around 10^{-8} [$m^3/(Pa{\cdot}m^2)$], while for two-phase reservoirs they are on the order of 10^{-5} [$m^3/(Pa{\cdot}m^2)$]; and skin factor s in Icelandic geothermal reservoirs is commonly between –3 and –1, although values may range from about –5 to 20.

5. PRODUCTION WELL TESTS

5.1 Theoretical background on discharge testing methods

Production well tests are conducted to determine the energy content (deliverability) and to analyse the flow characteristics of a well. The tests are done by measuring the fluid flow from a discharging well at different wellhead pressures (or lip pressures). The common practise for high-enthalpy wells is to conduct the discharge tests after the wells have been allowed to heat up for 2-4 months (Grant et al., 1982 and Jónsson, 2010). The warming up period ensures that the well has already attained the maximum possible temperatures and pressures as it would in undisturbed natural state. After the long hours of cold water injections during drilling and other injection activities, the temperature and pressure conditions in the geothermal reservoir in the vicinity of the well are altered significantly. Therefore, any production tests conducted prior to proper warm up of the well would not reflect the correct energy state of the system.

Grant et al. (1982) stated that during production well tests a well is opened up and allowed to flow to the atmosphere. High-temperature wells are usually discharged into a silencer which also acts as a steam-water separator at atmospheric pressure. The main parameters measured during such tests are total flow rate, wellhead pressure and enthalpy of the fluid and steam/water fraction. Temperature of the fluid discharged, non-condensable gas content, and depth to water levels are also monitored. There are two main methods commonly applied for determining these parameters: the separator method and the lip pressure method. A brief explanation of these two methods is given below (Grant et al., 1982).

The separator method is the most reliable method for measuring flow. A separator is used to separate steam and water at a specific separator pressure so that the flow rate of each component of flow could be measured with an orifice plate (for water) and differential pressure sensor (for steam). The flow rate of water, W [kg/s], through an orifice is given by:

$$W = C\sqrt{\Delta P / v} \tag{6}$$

where C = The orifice constant, depends on setup and units;
ΔP = Differential pressure (bar);
v = Specific volume of fluid (m^3/kg).

The Lip pressure method is based on an empirical formula developed by Russell James (James, 1970). This method is not as accurate as the separator method but offers the advantages of minimum instrumentation requirements for the flow measurements. In the lip pressure method approach, the steam-water mixture from the well is discharged through a pipe into a silencer to separate the steam and water at atmospheric pressure. The lip pressure (the pressure of the fluid passing at the extreme end of the pipe) is measured with a gauge and the water flow from the silencer is measured using a sharp-edged weir near the silencer outlet (Grant et al., 1982). James's formula which is practically tested over enthalpy ranges of 400-2800 kJ/kg is given by:

$$\frac{GH_t^{1.102}}{P_{lip}^{0.96}} = 1680, G = W/A \tag{7}$$

where P_{lip} = The lip pressure in MP_a (if the unit of P_{lip} is bar-a then the constant 1680 in the right of Equation 7 should be 1,835,000);
G = The mass flow per unit area in kg/(s cm^2); and
H_t = Total enthalpy (kJ/kg).

The water flow rate (W_w) from the silencer is related to the total mass flow by:

$$\frac{Ww}{AP_{lip}^{0.96}} = \frac{1680}{H_t^{1.102}} \frac{H_s - H_t}{H_{sw}} \tag{8}$$

where H_s and H_w are steam and water enthalpies evaluated at separator or atmospheric pressure.

If separation is at atmospheric pressure of 100 k Pa (near sea level):

$$\frac{Ww}{AP_{lip}^{0.96}} = Y = \frac{0.74(2675 - H_t)}{H_t^{1.102}} \tag{9}$$

where A = The area of the discharge pipe (cm^2);
P_{lip} = The lip pressure (MPa) ; and
W_w = Water flow rate (kg/s).

Equation 9 can be solved for total enthalpy as:

$$H_t = \frac{2675 + 365Y}{1 + 3.1Y} \tag{10}$$

Total mass flow can also be calculated by:

$$X = \frac{H_t - H_w}{H_{sw}}, \; W = \frac{W_w}{1 - X} = \frac{W_w H_{sw}}{H_s - H_t} \tag{11}$$

5.2 Characteristic well curves of the boreholes in Hverahlíd

The most important outcome of production well tests is determining the characteristic well curves (output curves) of a production well. Two basic types of production (flow) tests may be done, output (deliverability) tests and run-down (transient) tests (Grant et al., 1982). In the case of run-down tests, pressure or flow is held constant and changes in flow or pressure (respectively) with time are measured over months or years. The output test involves measuring the flow characteristics parameters such as total flow rate, total enthalpy, steam (water) fraction by varying discharge pressures or flow rates over a short period of time (hours to days). The collected data from the output tests is analysed and plotted to determine the right characteristic well curves (also called output curves). These curves show how much energy (in terms of enthalpy or wellhead pressures) can be delivered by a producing well at different flow rates. The characteristic well curves are crucially required to set the operating parameters of power plants and to assess the reservoir. In this section, the characteristic well curves of HE-21, HE-36, HE-53 and HE-54 are discussed.

Reykjavik Energy has conducted production well tests for boreholes HE-21, HE-36, HE-53 and HE-54 (Sigfússon et al., 2010) and the reported characteristic well curves are shown in Figure 22. The data obtained was only in the form of plotted characteristic well curve report. The plots shown here are nothing more than reproductions of the original individual characteristic curve plots of each borehole that were done by Reykjavik Energy (Sigfússon et al., 2010).

In Figure 22, the characteristic well curve for HE-21 shows a more or less flat trend, meaning that total flow rate remains constant for varying wellhead pressures. A small range of wellhead pressure vs. total flow rate plot is shown compared to the plot of the other wells. If not arising from limitations in the test due to complications at the measuring site, the flat trend indicates that the well has limited production (deliverability) with about only 25 kg/s of maximum total flow rate at a maximum well head pressure of about 33 bar. Decreasing or increasing this wellhead pressure will not make much difference in the amount of total fluid flow discharged. HE-36 shows a better output curve than HE-21. It has maximum discharging pressure - MDP (the maximum pressure that can be attained by

throttling the well) of about 33 bars at near 0 kg/s of discharge. This value decreases linearly up to total flow values of about 55 kg/s beyond which the wellhead pressure starts to decrease drastically with increasing flow rates and becomes constant at 63 kg/s flow rate. This means that the well has attained its maximum flow rate at about 63 kg/s and there will be no more discharge that can be obtained even if the wellhead is opened to its fullest. The characteristic well curve of HE-53 shows wide variability of the output parameters ranging from about 100 bar pressure at closed well conditions (0 kg/s of total flow rate) to about 9 bars of wellhead pressure at maximum discharges of about 95 kg/s. This trend gives a wide range of options for wellhead pressure-flow rate based designs like in setting the design for a power plant. The well is reported to be one of the best producers in the Hellisheidi area and the characteristic well curve shows how powerful the well is. It is a characteristic curve for wells feeding from a reservoir of high permeability and increased reservoir pressures (Grant et al., 1982). The high wellhead pressures under closed well conditions also pose serious risks of accidents, and care must be taken when operating the well for different purposes such as conducting downhole measurements.

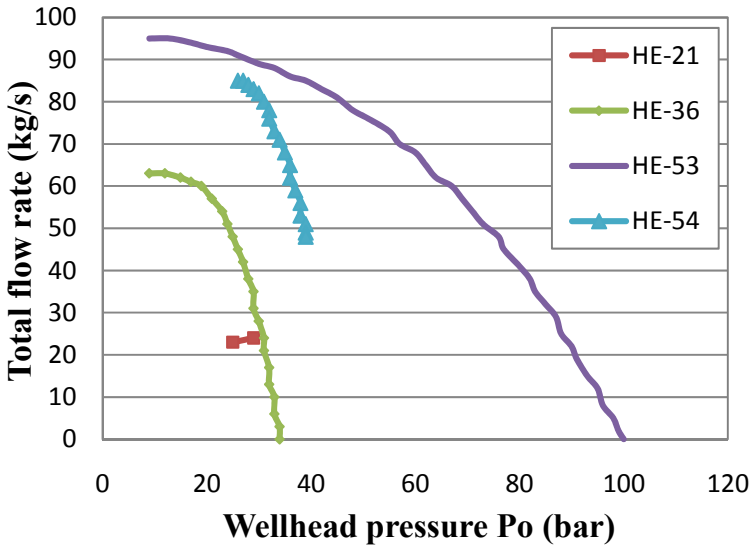

FIGURE 22: Characteristic well curves of HE-21, HE-36, HE-53 and HE-54 (data courtesy of Reykjavik Energy, modified from Sigfússon et al., 2010)

The characteristic well curve of HE-54 shows a fairly similar trend as HE-53 but with much lower wellhead pressure and total flow rate values. The curve starts at 39 bar, 48 kg/s and shows a more or less parabolic trend up to the point of 26 bar, 85 kg/s. Above 80 kg/s flow rate the curve appears to be flattening indicating that the well is approaching its maximum discharge capacity at slightly over 85 kg/s flow rate.

At low flow rates resistance to flow in either the wellbore or the reservoir itself becomes unimportant, and the flow depends only on the reservoir pressures and enthalpy (Grant et al., 1982). The best way to analyse this is the maximum discharging pressure (MDP). In 1980, Russell James proposed that there was a simple correlation between the MDP and discharge enthalpy given by:

$$T = 100P^{0.283} \tag{12}$$

where T is the temperature of the feed water from the reservoir (°C), and P is the MDP (bar).

This equation assumes the reservoir contains liquid water with no gas, the reservoir water level is at ground surface, and the reservoir follows a boiling point depth curve. Using this formula, the case of HE-53 was analysed. HE-53 has a single pivot point at 1260 m depth, with 97 bar pressure, an estimated formation temperature of 315°C and a boiling point depth temperature of about 310°C (Section 3.3). The calculated temperature using Equation 12 is about 368°C. If the pivot point values represent the best feed zone temperature in HE-53, then this estimate seems to be offset by about 50°C. However, considering the roughness of the estimations and all the complications involved in the real reservoir conditions, the estimation gives a rough idea on expected temperature conditions in the feed zones.

6. CONCLUSIONS AND RECOMMENDATIONS

The main goal of this project was to analyse the temperature and pressure characteristics of the Hverahlíd geothermal field based on data from four boreholes. Analyses of temperature and pressure profiles as well as injection well test analysis were the main methodologies applied in characterising the various aspects of the geothermal field. Some reports of geological and surface geophysical studies conducted in the area were also looked at to understand the overall geo-hydrological characteristics of the geothermal field. The characteristic well curves (output curves) of the boreholes were also reviewed to provide an appreciation of the production capacity (deliverability) of the boreholes in the study area. The following conclusions can be made from the combined observations of the aforementioned analysis.

1) The Hverahlíd field is a high-temperature geothermal field with formation temperatures of up to more than 300°C and more than 85 bar pressure at feed zones. Measured bottom-hole pressures are generally in excess of 150 bars.
2) The temperature profiles show that the main inflow of water is concentrated at three major feed zones. The depth to these feed zones could be slightly different in the boreholes, but they are usually found at the depth ranges of 700-900, 1000-1300 and 1800-2000 m. Other minor feed zones are also present at various depths in the boreholes. Some of the feed zones are connected to each other by cross flow. This can be readily deduced from the convective heat flow patterns observed in most temperature profiles in the boreholes.
3) The formation temperature profiles show that in most cases the geothermal reservoir at Hverahlíd is in boiling conditions. Two-phase flow scenarios prevail in the field, in some instances with dry steam conditions.
4) The temperature distribution as inferred from a two-dimensional cross-section across the area shows a probable upflow zone in the middle of the area (between boreholes HE-53 and HE-54). Fracture controlled northwest directed lateral hot geothermal fluid flow is also possible. In general, the area south of the boreholes seems to be the most productive zone. The boreholes targeting mainly this part of the field (HE-53 and HE-54) happen to be among the best wells in the area. Future geothermal exploration in the area might need to focus around this zone.
5) The well test analysis results show that the reservoir is generally characterised by good permeability and storativity. Generally, above average values of the injectivity index are also observed. The observed pressure responses are not very high even with high injection rates. This is an indication of how open the reservoir system is, in which high permeability with abundant fracture controlled flows prevail.
6) Analysis of the characteristic well curves of the boreholes shows boreholes HE-53 and HE-54 are characterised by high production capacities. Boreholes HE-21 and HE-36 are relatively less powerful. This has also been inferred from the temperature profiles and well test analysis results.
7) The results of the analysis show the presence of good combinations of reservoir parameters for sustainable geothermal development in the area.

ACKNOWLEDGEMENTS

I would like to express my sincere gratitude to my supervisors Svanbjörg H. Haraldsdóttir, Páll Jónsson and Saeunn Halldórsdóttir whose invaluable assistance and guidance has made it possible for this report to be completed successfully. Hjalti Franzson gave comments on the geology besides assisting with providing data for the project from Orkuveita Reykjavíkur (Reykjavík Energy), who in turn gave their permission willingly. I also thank all the UNU-GTP staff members and all the lecturers who have been involved in giving us all the knowledge and training to achieve our goals during the six months training programme. I also appreciate all the help and assistance that my UNU-GTP 2010 colleagues offered and for their continued friendship during my stay in Iceland.

REFERENCES

Arason, Th., Björnsson, G., Axelsson, G., Bjarnason, J.Ö., and Helgason, P., 2004: *ICEBOX – geothermal reservoir engineering software for Windows. A user's manual.* ISOR, Reykjavík, report 2004/014, 80 pp.

Árnason, K., Eysteinsson, H., Hersir, G.P., 2010: Joint 1D inversion of TEM and MT data and 3D inversion of MT data in the Hengill area, SW Iceland. *Geothermics, 39*, 13–34.

Björnsson, G., 2004: Reservoir conditions at 3-6 km depth in the Hellisheidi geothermal field, SW-Iceland, estimated by deep drilling, cold water injection and seismic monitoring. *Proceedings of the 29th Workshop on Geothermal Reservoir Engineering, Stanford University, Stanford, Ca,* 8 pp.

Elíasson, J., and Kjaran, S.P., 1983: *Geothermal reservoir engineering lecture notes*. UNU-GTP, Iceland report 2, 250 pp.

Franzson, H., Gunnlaugsson, E., Árnason, K., Saemundsson, K., Steingrímsson, B., and Hardarson, B.S., 2010: The Hengill geothermal system, conceptual model and thermal evolution. *Proceedings of the World Geothermal Congress 2010, Bali, Indonesia,* 9 pp.

Franzson, H., Kristjánsson, B.R., Gunnarsson, G., Björnsson, G., Hjartarson, A., Steingrímsson, B., Gunnlaugsson, E., and Gíslason G., 2005: The Hengill-Hellisheidi geothermal field. Development of a conceptual geothermal model. *Proceedings World Geothermal Congress 2005, Antalya, Turkey,* CD, 7 pp.

Grant, M.A., Donaldson, I.G., and Bixley, P.F., 1982: *Geothermal reservoir engineering*. Academic Press, New York, 369 pp.

Hardarson, B.S., Einarsson, G.M., Kristjánsson, B.R., Gunnarsson, G., Helgadóttir, HM., Franzson, H., Árnason, K., Ágústsson, K., and Gunnlaugsson, E., 2010: Geothermal reinjection at the Hengill triple junction, SW Iceland. *Proceedings of the World Geothermal Congress 2010, Bali, Indonesia*, 7 pp.

Helgadóttir, H.M., Snaebjörnsdóttir, S, Níelsson, S., Gunnarsdóttir S.H., Theódóra, M., Hardarson, B.S., Einarsson, G.M., and Franzson, H., 2010 : Geology and hydrothermal alteration in the reservoir of the Hellisheidi high temperature system, SW-Iceland. *Proceedings* of the *World Geothermal Congress 2010, Bali, Indonesia,* 10 pp.

Hjartarson, A., 1999: *Analysis of reservoir data collected during reinjection into the Laugaland geothermal system in Eyjafjördur, N-Iceland*. University of Iceland and Orkustofnun, MSc. thesis, Reykjavík, 107 pp.

Horne, R.N., 1995: *Modern well test analysis, A computer aided approach* (2nd ed). Petroway Inc., Palo Alto, 257 pp.

Iceland on the Web, 2010: *Geology of Iceland.* Iceland on the Web, website: *iceland.vefur.is/Iceland_nature/Geology_of_Iceland/index.htm.*

James, R., 1970: Factors controlling borehole performance. *Geothermics, Sp. Issue, 2-2,* 1502-1515.

Jónsson, P., 2010: Injection well testing. UNU/GTP 2010, unpublished lecture notes, 56 pp.

Júlíusson, E., Grétarsson, G.J., and Jónsson, P., 2008: *WellTester 1.0b user´s guide.* ÍSOR, Reykjavík, report ÍSOR-2008/063, 27 pp.

Matthíasdóttir, T., Sigurgeirsson, M.Á., Björnsson, H., and Ingólfsson, H., 2010: *Hverahlíd – borehole HE-54, 3rd stage: Drilling for the production part from 759 m to 2436 m depth for a 7" liner*. ÍSOR, Reykjavík, report ÍSOR-2010/010, 78 pp.

Mortensen, A.K., Egilsson, Th., Franzson, H., Richter, B., Ásmundsson, R.K., Danielssen, P.E., Steingrímsson, B., and Thórisson, S., 2006: *Hverahlíd – borehole HE-21, 3rd stage: Drilling of production part from 300 m to 903 m depth for an 8½" liner.* ÍSOR, Reykjavík, report ÍSOR-2006/018, 79 pp.

Níelsson, S., and Franzson, H., 2010: Geology and hydrothermal alteration of the Hverahlíd HT-system, SW-Iceland. *Proceedings of the World Geothermal Congress 2010, Bali, Indonesia*, 6 pp.

Níelsson, S., and Haraldsdóttir, S.H., 2008: *Hverahlíd – borehole HE-36, 3rd stage: Drilling of production part from 1104 m to 2808 m with 8½" drill bit.* ÍSOR, Reykjavík, report, ISOR-2008/046, 173 pp.

Saemundsson, K., 1995: *Geological map of the Hengill area 1:50,000*. Orkustofnun, Reykjavík.

Sigfússon, B., Kjartansson, G., and Ásbjörnsson, E.J., 2010: *Power and productivity of high temperature geothermal wells at Hellisheidi.* Reykjavik Energy, report 2010-1.